Supplementary report: Is RaTG13 specifically adapted to a restriction scar sequence? Effect of the BamHI restriction scar on the binding of the RaTG13 RBD to ACE2 of humans and bats deduced through a literature review of 9 articles.

Article 1:

SARS-CoV-2 Spike Affinity and Dynamics Exclude the Strict Requirement of an Intermediate Host

Matteo Castelli, Luigi Scietti, Nicola Clementi, Mattia Cavallaro, Silvia Faravelli, Alberta Pinnola, Elena Criscuolo, Roberta
Antonia Diotti, Massimo Clementi, Federico Forneris, Nicasio Mancini

bioRxiv 2021.08.11.455960; doi: https://doi.org/10.1101/2021.08.11.455960

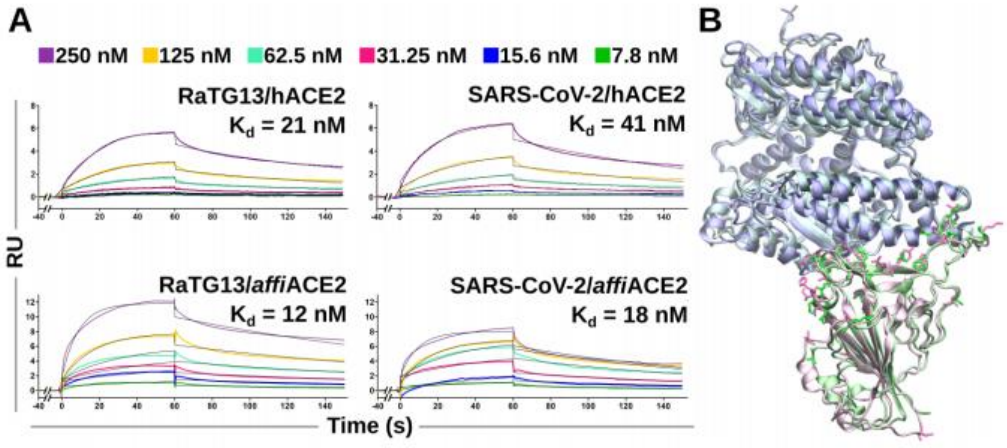

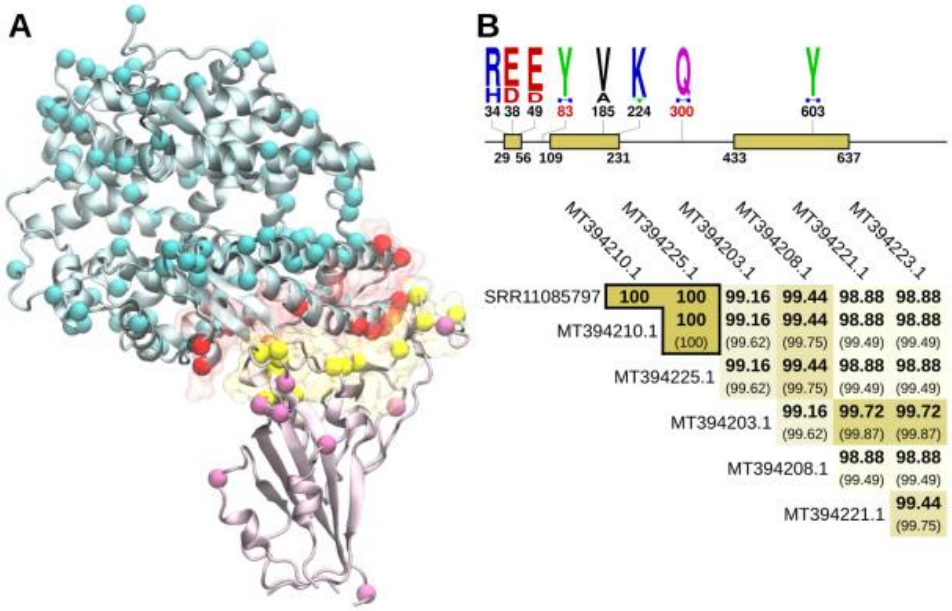

Claim:

" Surprisingly, we found that both RBDs bind to hACE2 with Kd in the nanomolar range (21 and 41 nM, respectively) (Fig. 2A)."

Method section:

"Generation of plasmid vectors for recombinant protein production. The pCAGGS plasmids for production of the C-terminal His-tagged SARS-CoV-2 S protein (#NR_52310) and RBD (#NR_52310), were obtained from BEIRESOURCES (NY, USA). The designed codon-optimized sequence encoding for RaTG13 RBD and the cDNA for affiACE2 ectodomain (residue 19-615, based on the sequence deposited on Genbank under the ID MT394225.1) were synthesized by Genewiz with flanking 5'-BamHI and 3'-NotI restriction sites and sub-cloned into pUPE.107.03 plasmid vectors (U-Protein Express B.V., The Netherlands) providing the human cystatin protein signal peptide and C-terminal 6xHistag for purification. The cDNA for hACE2 ectodomain was obtained from AddGene (#141185). The sequence was amplified using PCR with oligonucleotides hACE2ecto-Fw (5'-aaaatgatcaTCCACCATTGAGGAACAGGCC-3') and hACE2ecto_Rv (5'- aaaagcggccgcGTCTGCATATGGACTCCAGTC-3') and sub-cloned into a pUPE.06.45 expression vector (U-Protein Express B.V., The Netherlands) providing the signal sequence from cystatin followed by a removable (TEV-cleavable) N-terminal 6xHis-Strep-tag."

Article 2:

Kefang Liu, Xiaoqian Pan, Linjie Li, Feng Yu, Anqi Zheng, Pei Du, Pengcheng Han, Yumin Meng, Yanfang Zhang, Lili Wu, Qian Chen, Chunli Song, Yunfei Jia, Sheng Niu, Dan Lu, Chengpeng Qiao, Zhihai Chen, Dongli Ma, Xiaopeng Ma, Shuguang Tan, Xin Zhao, Jianxun Qi, George F. Gao, Qihui Wang,
Binding and molecular basis of the bat coronavirus RaTG13 virus to ACE2 in humans and other species,
Cell,
Volume 184, Issue 13,
2021,
Pages 3438-3451.e10,
ISSN 0092-8674,
https://doi.org/10.1016/j.cell.2021.05.031.
(https://www.sciencedirect.com/science/article/pii/S0092867421006619)

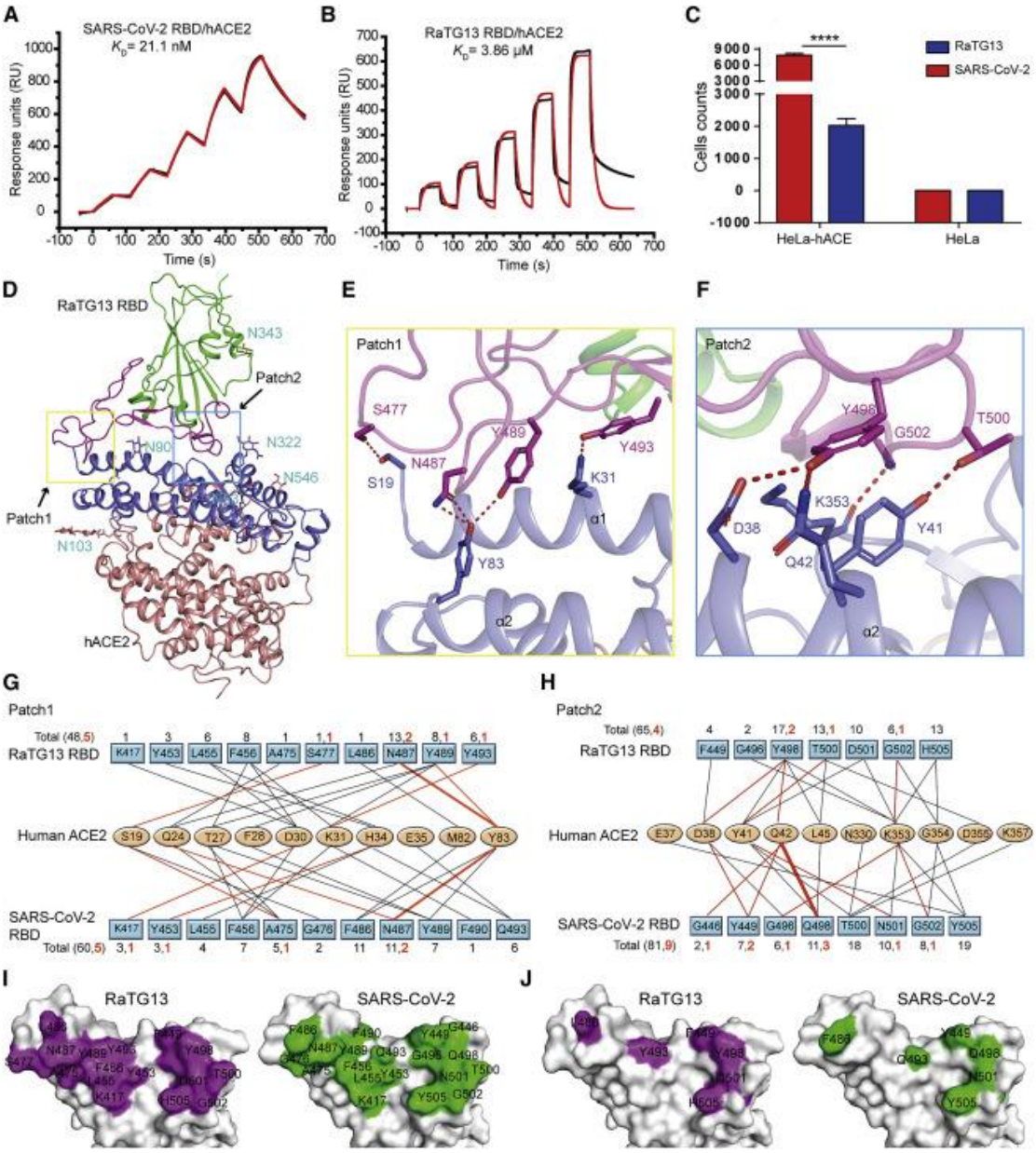
A
SARS-CoV-2 RBD/hACE2
K_D= 21.1 nM
Response units (RU)
Time (s)
B
RaTG13 RBD/hACE2
K_D= 3.86 μM
Response units (RU)
Time (s)
C
****
RaTG13
SARS-CoV-2
Cells counts
HeLa-hACE
HeLa
D
RaTG13 RBD
N343
Patch2
N322
N80
N546
Patch1
N103
hACE2
E
Patch1
S477
Y489
Y493
N487
S19
K31
α1
Y83
α2
F
Patch2
Y498
G502
T500
K353
D38
Y41
Q42
α2
G
Patch1
Total (48,5)
RaTG13 RBD
K417 Y453 L455 F456 A475 S477 L486 N487 Y489 Y493
Human ACE2
S19 Q24 T27 F28 D30 K31 H34 E35 M82 Y83
SARS-CoV-2 RBD
K417 Y453 L455 F456 A475 G476 F486 N487 Y489 F490 Q493
Total (60,5)
H
Patch2
Total (65,4)
RaTG13 RBD
F449 G496 Y498 T500 D501 G502 H505
Human ACE2
E37 D38 Y41 Q42 L45 N330 K353 G354 D355 K357
SARS-CoV-2 RBD
G446 Y449 G498 Q498 T500 N501 G502 Y505
Total (81,9)
I
RaTG13
SARS-CoV-2
J
RaTG13
SARS-CoV-2

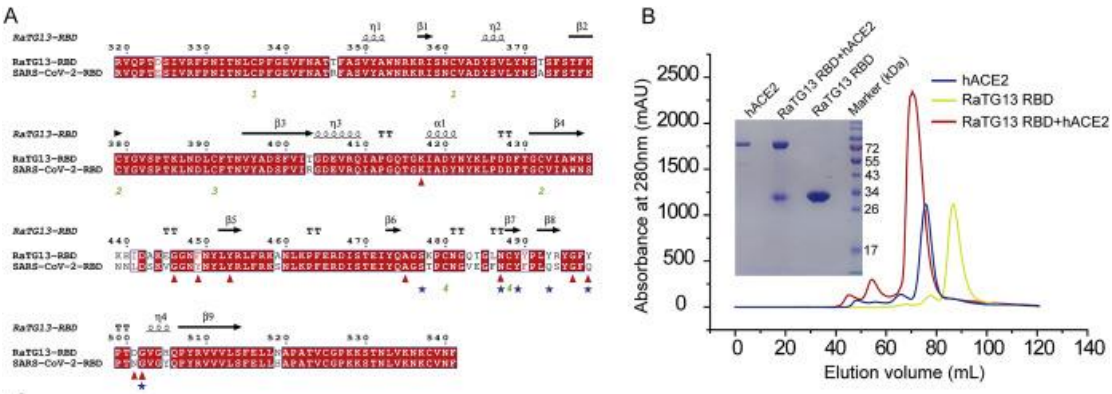

C

	P1 19	P1 24	P1 27	P1 28	P1 30	P1 31	P1 34	P2 38	P2 41	P2 42	P2 45	P1 82	P1 83	P2 353	P2 354	P2 355	Substitutions	
Human	S	Q	T	F	D	K	H	D	Y	Q	L	M	Y	K	G	D		Primates
Macaca	S	Q	T	F	D	K	H	D	Y	Q	L	M	Y	K	G	D	0	
Rabbit	S	L	T	F	E	K	Q	D	Y	Q	L	T	Y	K	G	D	4	Lagomorpha
Mouse	S	N	T	F	N	N	Q	D	Y	Q	L	S	F	H	G	D	7	Rodentia
Rat	S	K	S	F	N	K	Q	D	Y	Q	L	N	F	H	G	D	7	
Malayan pangolin	S	E	T	F	E	K	S	E	Y	Q	L	N	Y	K	H	D	6	Pholidota
Cat	S	L	T	F	E	K	H	E	Y	Q	L	T	Y	K	G	D	4	
Civet	S	L	T	F	E	T	Y	E	Y	Q	V	T	Y	K	G	D	7	
Fox	S	L	T	F	E	K	Y	E	Y	Q	L	T	Y	K	G	D	5	Carnivora
Dog	S	L	T	F	E	K	Y	E	Y	Q	L	T	Y	K	G	D	5	
Raccoon dog	S	L	T	F	E	K	Y	E	Y	Q	L	T	Y	R	G	D	6	
Horse	S	L	T	F	E	K	S	E	H	Q	L	T	Y	K	G	D	6	Perissodactyla
Pig	F	L	T	F	E	K	L	D	Y	Q	L	T	Y	K	G	D	5	
Wild bactrian camel	S	L	T	F	E	E	H	D	Y	Q	L	T	Y	K	G	D	4	
Alpaca	S	L	T	F	K	E	H	D	Y	Q	L	I	Y	K	G	D	4	Artiodactyla
Bovine	S	Q	T	F	E	K	H	D	Y	Q	L	T	Y	K	G	D	2	
Goat	S	Q	T	F	E	K	H	D	Y	Q	L	T	Y	K	G	D	2	
Sheep	S	Q	T	F	E	K	H	D	Y	Q	L	T	Y	K	G	D	2	
Little brown bat	S	K	I	F	E	N	S	D	H	E	L	T	Y	K	G	D	8	
Intermediate horseshoe bat	S	R	I	F	D	N	R	E	Y	Q	L	N	Y	K	G	D	6	
Fulvous fruit bat	S	L	T	F	E	K	T	D	Y	Q	L	T	Y	K	G	D	4	Chiroptera
Greater horseshoe bat	S	L	K	F	D	D	S	N	H	Q	L	N	F	K	G	D	8	
Least horseshoe bat	S	K	K	F	N	D	S	D	Y	Q	L	N	Y	K	G	D	6	
Big-eared horseshoe bat	S	E	K	F	D	K	S	D	Y	E	L	N	Y	K	G	D	5	
Lesser hedgehog tenrec	S	Q	S	F	T	T	N	N	Y	Q	L	K	F	L	N	D	9	Afrotheria

Result:

"The binding affinity between the RaTG13 RBD and hACE2 is approximately 70-fold lower than that between the SARS-CoV-2 RBD and hACE2 because of the substantially reduced area of the buried surface and decreased network of hydrogen bonds in the RaTG13 RBD-hACE2 complex structure. "

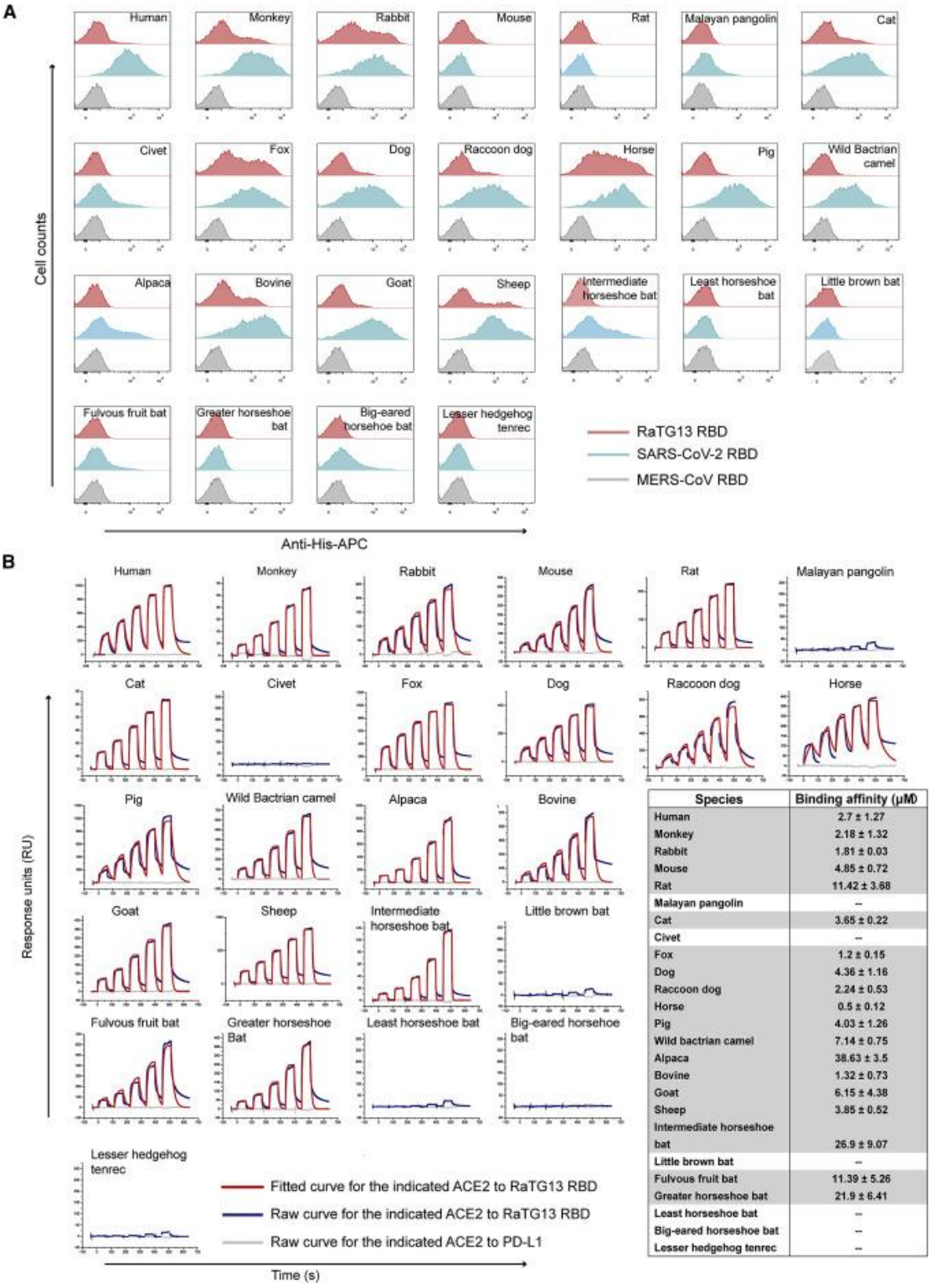

Species	Binding affinity (μM)
Human	2.7 ± 1.27
Monkey	2.18 ± 1.32
Rabbit	1.81 ± 0.03
Mouse	4.85 ± 0.72
Rat	11.42 ± 3.68
Malayan pangolin	--
Cat	3.65 ± 0.22
Civet	--
Fox	1.2 ± 0.15
Dog	4.36 ± 1.16
Raccoon dog	2.24 ± 0.53
Horse	0.5 ± 0.12
Pig	4.03 ± 1.26
Wild bactrian camel	7.14 ± 0.75
Alpaca	38.63 ± 3.5
Bovine	1.32 ± 0.73
Goat	6.15 ± 4.38
Sheep	3.85 ± 0.52
Intermediate horseshoe bat	26.9 ± 9.07
Little brown bat	--
Fulvous fruit bat	11.39 ± 5.26
Greater horseshoe bat	21.9 ± 6.41
Least horseshoe bat	--
Big-eared horseshoe bat	--
Lesser hedgehog tenrec	--

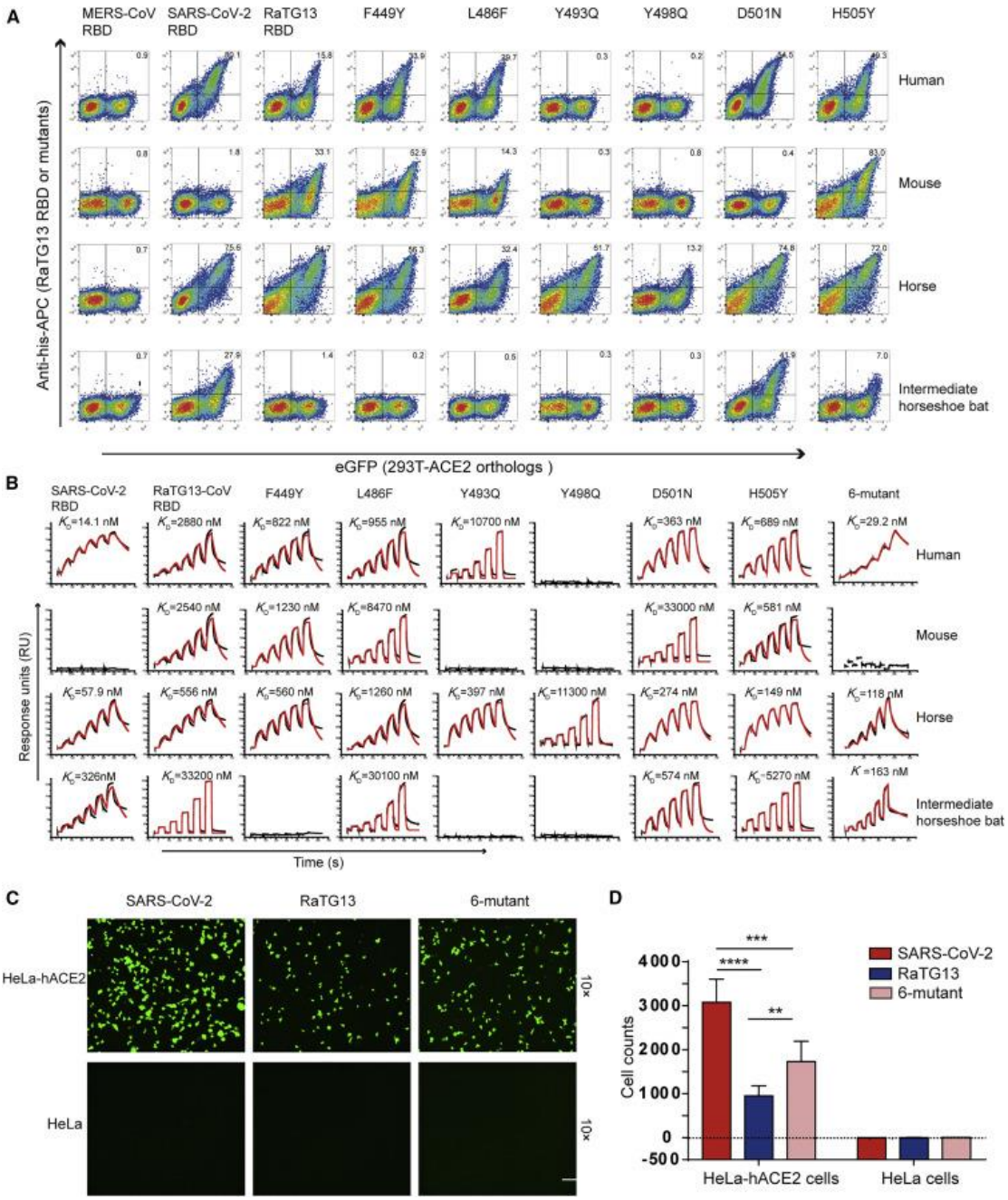

"The RaTG13 RBD was capable of binding to human, monkey, rabbit, cat, fox, dog, raccoon dog, horse, pig, bovine, wild Bactrian camel, goat, sheep, and mouse ACE2, with equilibrium dissociation constant (KD) values of 0.5–7.14 μM, but were unable to interact with Malayan pangolin, civet, little brown bat, least horseshoe bat, big-eared horseshoe bat, or lesser hedgehog tenrec ACE2s (Figure 2B)."

Method section

Gene cloning

The full-length coding sequence of the 25 ACE2 orthologs was synthesized and cloned into the pEGFP-N1 vector for flow cytometry (Table S1). The extracellular domain of these 25 ACE2

orthologs fused with the Fc domain of mouse IgG (mFc) were cloned into the pCAGGS vector for protein expression. The coding sequences of RaTG13 RBD (residues 319-541, GenBank: QHR63300.2), SARS-CoV-2 RBD (residues 319-541, GISAID: EPI_ISL_402119), MERS-CoV RBD (residues 367-606, GenBank: JX869059) and hACE2 (residues 19-615, NCBI Reference Sequence: NP_001358344.1) were cloned into pFastBac vectors (Dai et al., 2020; Lu et al., 2013). The wild-type RaTG13 RBD (residues 319-541, GenBank: QHR63300.2) and mutated RaTG13 RBDs (F449Y, L486F, Q493Y, Q498Y, D501N and H505Y) were cloned in pCAGGS vectors. The coding sequence of RaTG13 S (residues 1-1233) and SARS-CoV-2 S (residues 1-1255) were cloned into pCAGGS vectors. The variable region of MAbs, REGN10933 (PDB: 6XDG), REGN10987 (PDB: 6XDG), C110 (PDB: 7K8P), and S2H14 (PDB: 4JX3) fused with the constant region of IgG1 were cloned into pCAGGS vectors. The extracellular domain of PD-L1 was constructed as previously described.

Table S1. The coding genes of 25 ACE2 orthologs, Related to Figure 2

Species of ACE2	Organism	Database	Code
Human	*Homo sapiens*	NCBI Reference Sequence	NP_001358344.1
Macaca	*Macaca fascicularis*	NCBI Reference Sequence	XP_005593094.1
Rabbit	*Oryctolagus cuniculus*	NCBI Reference Sequence	XP_002719891.1
Mouse	*Mus musculus*	NCBI Reference Sequence	NP_001123985.1
Rat	*Rattus norvegicus*	NCBI Reference Sequence	NP_001012006.1
Malayan pangolin	*Manis javanica*	NCBI Reference Sequence	XP_017505746.1
Cat	*Lynx canadensis*	NCBI Reference Sequence	XP_030160839.1
Civet	*Paguma larvata*	NCBI Reference Sequence	Q56NL1.1
Fox	*Vulpes vulpes*	NCBI Reference Sequence	XP_025842512.1
Dog	*Canis lupus familiaris*	NCBI Reference Sequence	XP_005641049.1
Raccon Dog	*Nyctereutes procyonoides*	GenBank	ABW16956.1
Horse	*Equus caballus*	NCBI Reference Sequence	XP_001490241.1
Pig	*Sus scrofa*	NCBI Reference Sequence	XP_020935033.1
Wild bactrian camel	*Camelus ferus*	NCBI Reference Sequence	XP_006194263.1
Alpaca	*Vicugna pacos*	NCBI Reference Sequence	XP_006212709.1
Bovine	*Bos taurus*	NCBI Reference Sequence	XP_005228486.1
Goat	*Capra hircus*	NCBI Reference Sequence	XP_005701129.2
Sheep	*Ovis aries*	NCBI Reference Sequence	XP_011961657.1
Intermediate horseshoe bat	*Rhinolophus affinis*	GenBank	QMQ39222.1
Little brown bat	*Myotis lucifugus*	NCBI Reference Sequence	XP_023609439.1
Fulvous fruit bat	*Rousettus leschenaultii*	GenBank	ADJ19219.1
Greater horseshoe bat	*Rhinolophus ferrumequinum*	NCBI Reference Sequence	BAH02663.1
Least horseshoe bat	*Rhinolophus pusillus*	GenBank	ADN93477.1
Big-eared horseshoe bat	*Rhinolophus macrotis*	GenBank	ADN93471.1
Lesser hedgehog tenrec	*Echinops telfairi*	NCBI Reference Sequence	XP_004710002.1

Article 3:

Guo H, Hu B, Si HR, Zhu Y, Zhang W, Li B, Li A, Geng R, Lin HF, Yang XL, Zhou P, Shi ZL. Identification of a novel lineage bat SARS-related coronaviruses that use bat ACE2 receptor. Emerg Microbes Infect. 2021 Dec;10(1):1507-1514. doi: 10.1080/22221751.2021.1956373. PMID: 34263709; PMCID: PMC8344244.

S

ACE2 / RBD	Human	*R.affinis*	Pangolin
SARS-CoV-2	1.00	>1.09	1.47
RaTG15	Not detectable	3.90	2.72
Pangolin-CoV-GD	2.28	1.13	0.05
Pangolin-CoV-GX	3.26	1.30	0.10
RaTG13	Low affinity, >3.53	16.57	7.61
SARS-CoV-1	9.07	6.19	2.88

T

		Human ACE2	Bat ACE2	Pangolin ACE2	Deletion 1	Deletion 2
SARS-CoV-1 related lineage	SARS-CoV-1	√	√	√		
	WIV16-CoV	√	√	ND		
	Rp3-CoV	×	×	ND	Y	Y
SARS-CoV-2 related lineage	SARS-CoV-2	√	√	√		
	RaTG13	weak	weak	weak		
	Rc-o0319	×	√	ND		Y, partial
	RmYN02	×	ND	ND	Y	Y
	RacCS213	×	ND	ND	Y	Y
	Pangolin-CoV-GX	√	√	√		
	Pangolin-CoV-GD	√	√	√		
Novel lineage	RaTG15	×	√	√	Y	

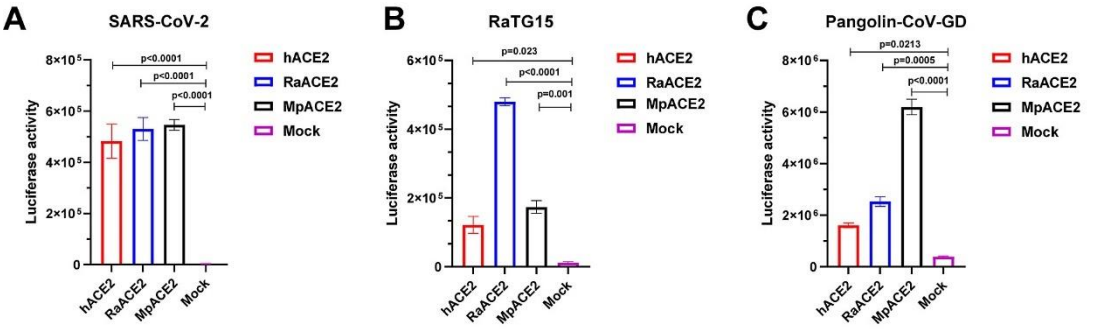

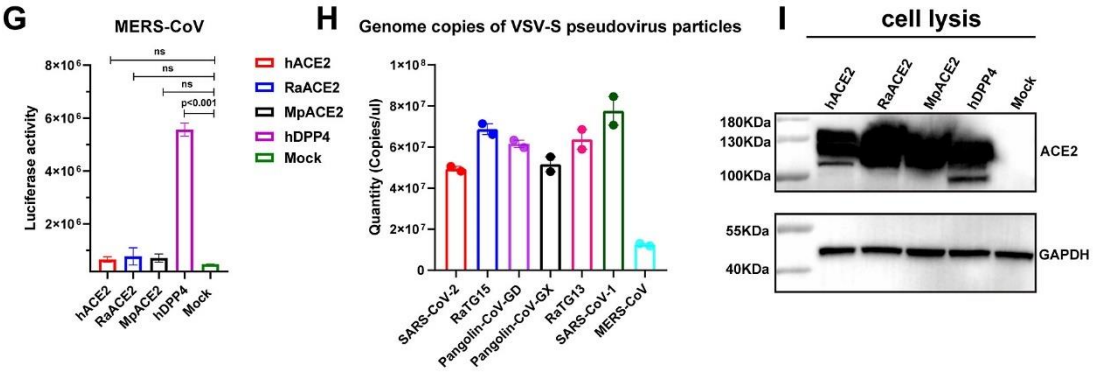

Claim:

“RaTG13 RBD showed very weak binding to RaACE2, MpACE2, and human ACE2 (Figure 3G-S and Figure S2B).”

Method section

“The ectodomains of human ACE2 (aa 19–615, accession number: AB046569), R. affinis ACE2 (aa 19–615, accession number: MT394204), and Malayan pangolin ACE2 (aa 19–615, accession number: XM_017650263.2) were amplified or synthesized, and cloned into the expression vector with an N-terminal signal peptide and C-terminal S-tag as described previously [15].”

Reference [15] of Article 3:

“[15] Guo H, Hu B-J, Yang X-L, et al. Evolutionary arms race between virus and host drives genetic diversity in bat severe acute respiratory syndrome-related coronavirus spike genes. J Virol. 2020;94(20): e00902–20.”

Method section:

“Amplification, cloning, and expression of bats ACE2 gene.

The bat ACE2 gene was amplified using DNA from the intestinal tissue of bats. In brief, total RNA was extracted from bat intestine tissue using the RNAprep Pure kit (for cell/bacteria) (Tiangen, Beijing, China). First-strand cDNA was synthesized from total RNA by reverse transcription with random hexamers; full-length bat ACE2 fragments were amplified by reverse transcription0nested PCR (RT-PCR). Primers were designed based on available ACE2 sequences from NCBI. The first-round primers wereF-ACE2-out-AATGGGGTTTTGGCGCTCAG and R-ACE2-out-CATACAATGAAATCACCTCAAGAG, and the second-round primers were F-ACE2-in-CAGGGAAAGATGTCAGGCTC and R-ACE2-in-TTCTAAAABGAVGTYTGAAC. The ACE2 gene was cloned into the pcDNA3.1 vector with XhoI and BamHI. N-terminal mouse Igk or human interferon alpha-1 (IFN-α1) signal peptide and an S tag were inserted. The plasmids were verified by sequencing. The expression of human and R. sinicus ACE2 was confirmed by Western blotting and immunofluorescence assay.”

“R. sinicus ACE2 (aa 19 to 615), human ACE2 (aa 19 to 615, accession number BAJ21180), and human DPP4 (aa 39 to 766, accession number NP_001926) into the expression vector, as described previously (65). For each protein, an N-terminal signal peptide and an S tag were added to facilitate protein secretion and purification.”

Article 4:

ACE2 binding is an ancestral and evolvable trait of sarbecoviruses

Tyler N. Starr, Samantha K. Zepeda, Alexandra C. Walls, Allison J. Greaney, David Veesler, Jesse D. Bloom

bioRxiv 2021.07.17.452804; doi: https://doi.org/10.1101/2021.07.17.452804

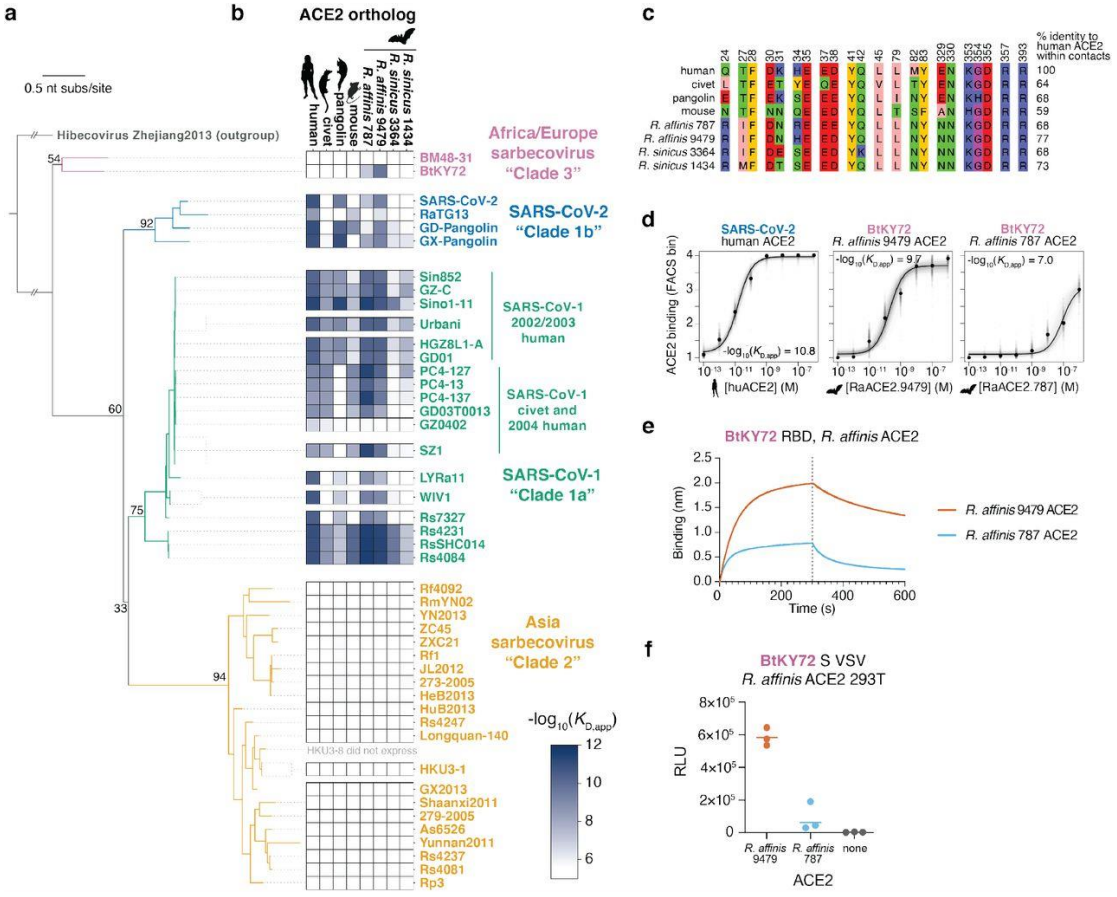

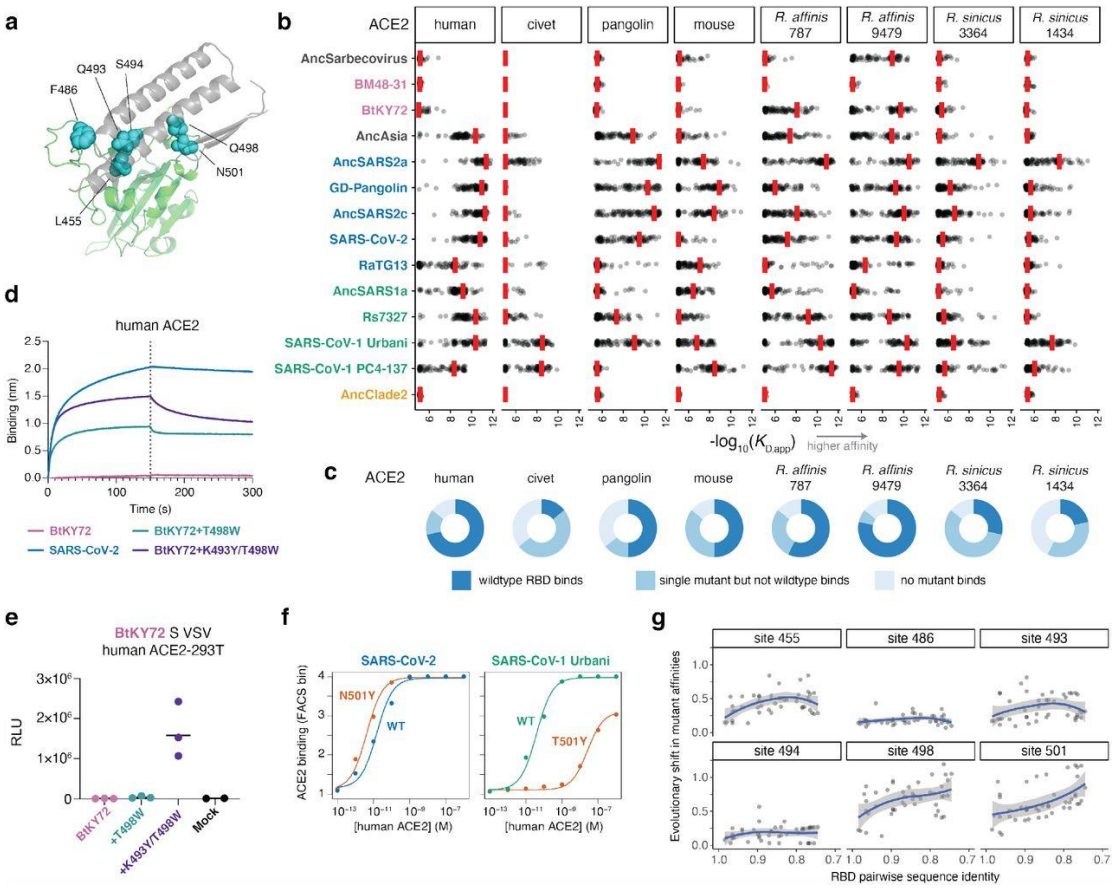

Results:

"However, the RBDs of the two viruses in our panel sampled from *R. affinis* bound only modestly (LYRa11) or very weakly (RaTG13) to the *R. affinis* alleles that we tested."

Methods section:

"The *R. affinis* 787 (GenBank: QMQ39222.1) and *R. affinis* 9479 (GenBank: QMQ39227.1) ACE2 ectodomains constructs were synthesized by GenScript and placed into a pCMV plasmid. The domain boundaries for the ectodomain are residues 19-615. The native signal tag was identified using SignalP-5.0 (residues 1-18) and replaced with a N-terminal mu-phosphatase signal peptide. These constructs were then fused to a sequence encoding thrombin cleavage site and a human Fc fragment at the C-terminal end."

Article 5:

"Mou H, Quinlan BD, Peng H, Liu G, Guo Y, Peng S, Zhang L, Davis-Gardner ME, Gardner MR, Crynen G, DeVaux LB, Voo ZX, Bailey CC, Alpert MD, Rader C, Gack MU, Choe H, Farzan M. Mutations derived from horseshoe bat ACE2 orthologs enhance ACE2-Fc neutralization of SARS-CoV-2. PLoS Pathog. 2021 Apr 9;17(4):e1009501. doi: 10.1371/journal.ppat.1009501. PMID: 33836016; PMCID: PMC8059821."

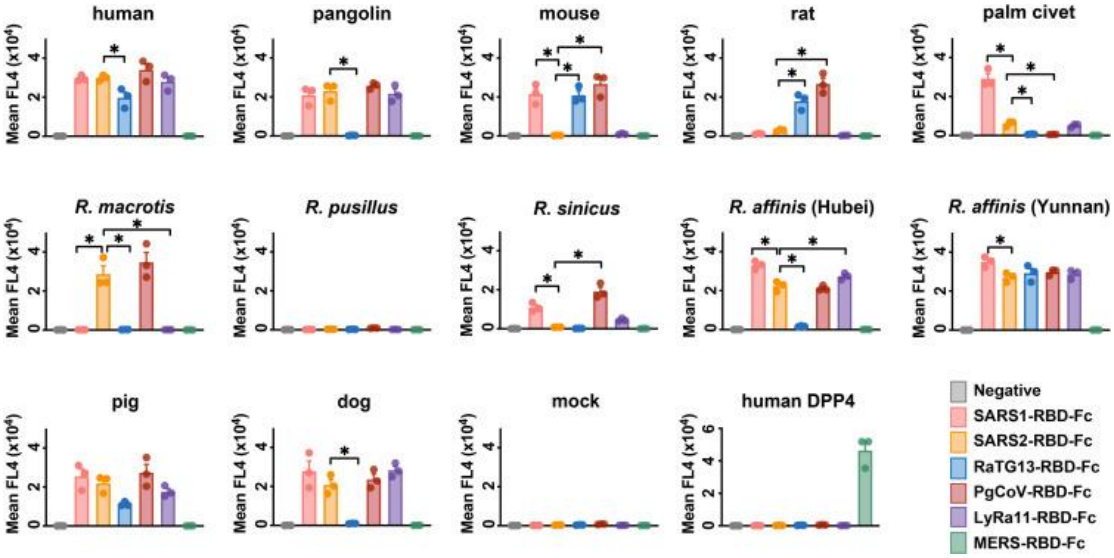

S1 Fig

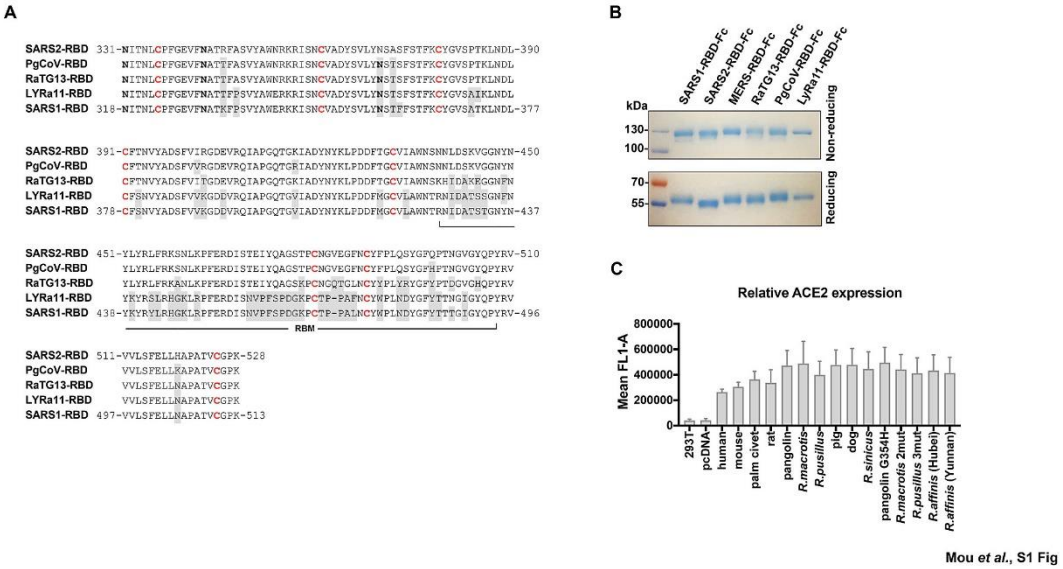

Mou *et al.*, S1 Fig

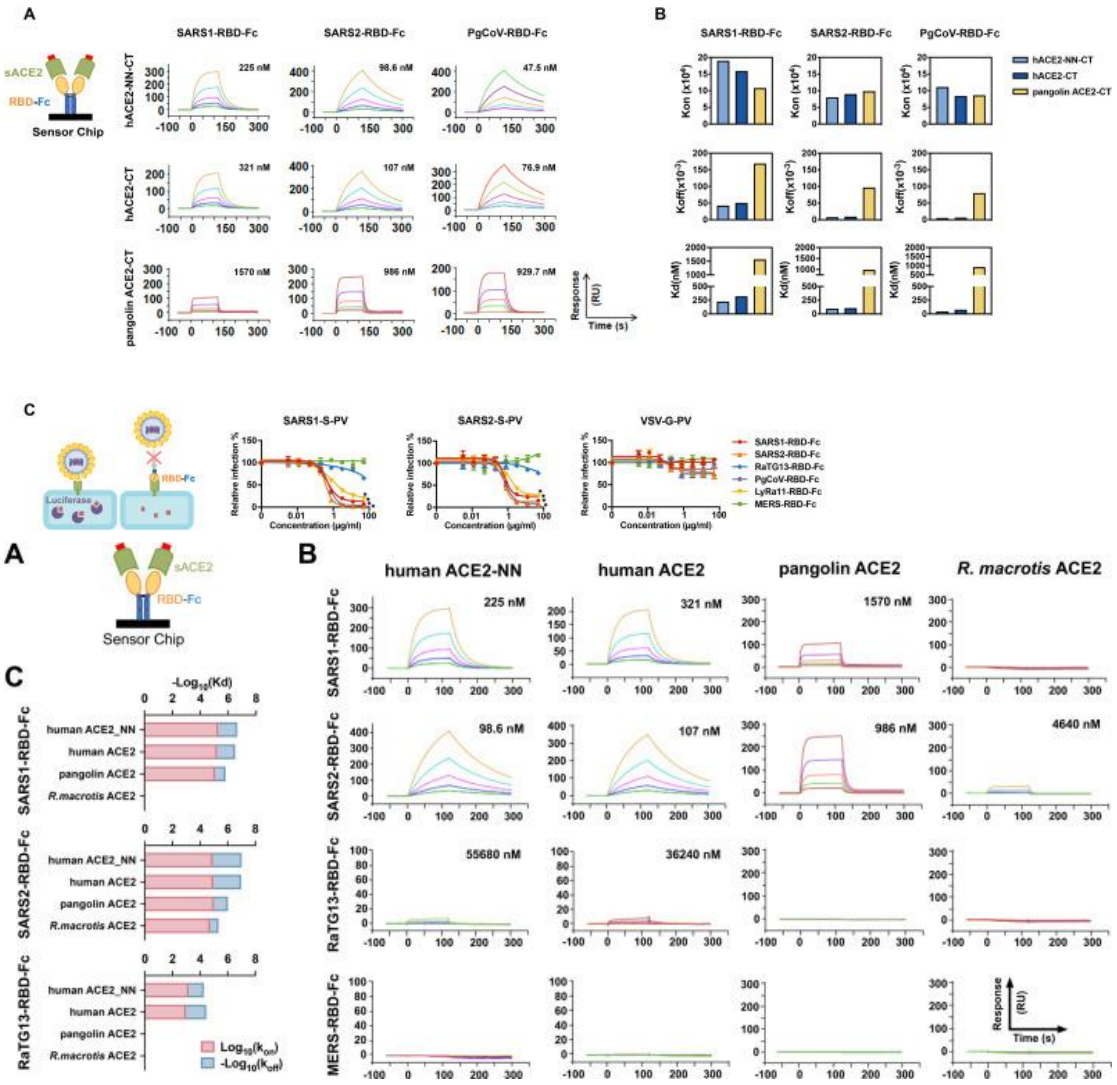

Results

Table: Normalized ACE2 binding compared to expression (mean.Fl4-A(RBD)/mean.Fl1-A(ACE2)

Mean. Fl-4A(ACE2)/Mean. Fl-1A(RBD)	SARS1	SARS2	RaTG13	PgCoV	LyRa11
Human	0.112692439	0.114779	0.075128	0.129388	0.106432
Mouse	0.070656371	0.001812	0.068845	0.088773	0.003623
Palm civet	0.081676172	0.016638	0.001513	0.001513	0.015125
Rat	0.001648649	0.008243	0.052757	0.080784	0.001649
pangolin	0.044118767	0.048763	0.001161	0.054568	0.046441
R.macrotis	0	0.058781	0	0.072612	0
R.Pusillus	0	0	0	0.001381	0
Pig	0.053406928	0.04528	0.02322	0.05689	0.035992
Dog	0.059212029	0.044119	0.002322	0.049924	0.059212

R.Sinicus	0.025131321	0.001257	0.001257	0.04398	0.010053
R.affinis (Hubei)	0.077133825	0.051423	0.003857	0.048851	0.062993
R.affinis (Yunnan)	0.084909412	0.064693	0.070084	0.071432	0.068736

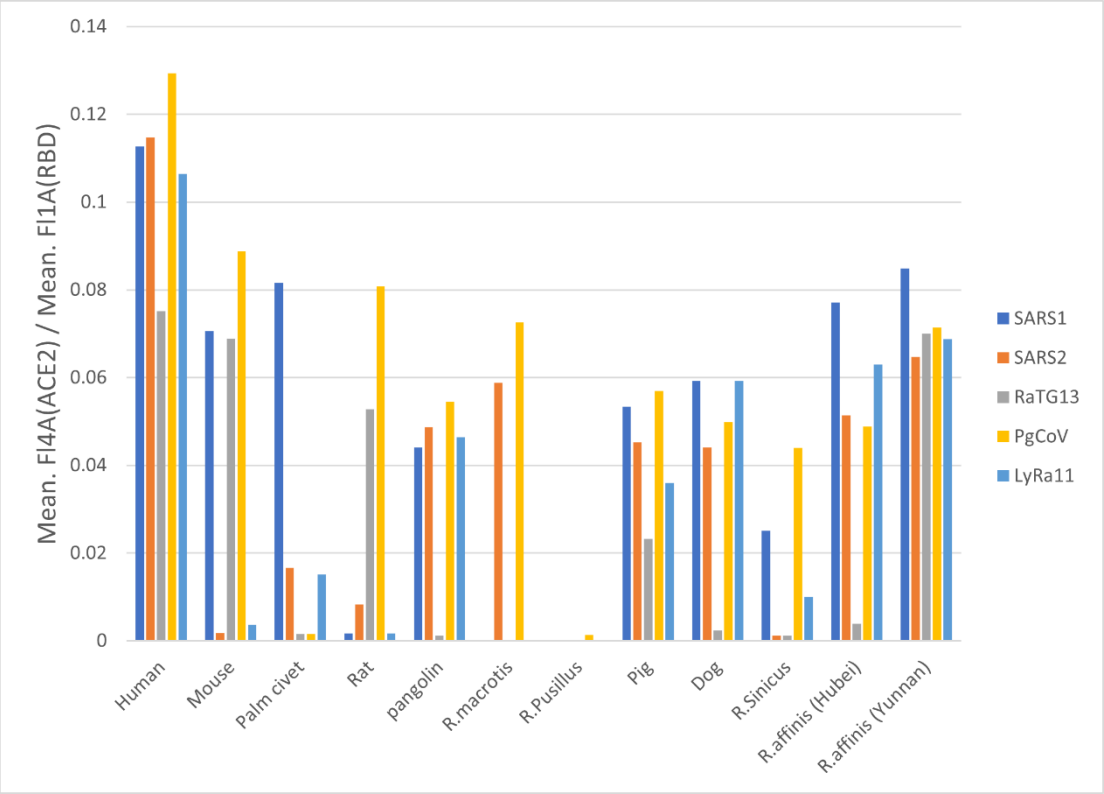

Figure: Normalized receptor binding for 4 RBD to ACE2 of various species

"The RaTG13-RBD bound only one of two *R. affinis* orthologs, despite having been found in this species, and no other bat ACE2 assayed."

Methods section:

S1 Table. Information for the expression plasmids used in this study.

	NCBI reference number	Vectors
human ACE2	BAB40370.1	pcDNA3.1
mouse ACE2	NP_001123985.1	pcDNA3.1
palm civet ACE2	AAX63775.1	pcDNA3.1
rat ACE2	NM_001012006.1	pcDNA3.1
pangolin ACE2	XM_017650257.1	pcDNA3.1
pig ACE2	NP_001116542.1	pcDNA3.1
Dog ACE2	NM_001165260.1	pcDNA3.1
***R. macrotis* ACE2**	ADN93471.1	pcDNA3.1
R. pusillus	ADN93477.1	pcDNA3.1
R. sinicus	ADN93475.1	pcDNA3.1
***R. affinis* (Hubei)**	MT394203.1	pcDNA3.1
***R. affinis* (Yunnan)**	MT394208.1	pcDNA3.1
human DPP4	AGF80256.1	pCG1
SARS1-S	NC_004718.3	pcDNA3.1
VSV-G	AJ318514.1	pCMV
SARS2-S and -RBD	QHD43416.1	pCAGGS
RaTG13-S and -RBD	QHR63300.1	pCAGGS
PgCoV-RBD	QIG55945.1	pCAGGS
MERS-RBD	YP_009047204.1	pCAGGS
LyRa-RBD	AHX37558.1	pCAGGS

“Plasmid

Protein sequence information used in this study was provided in **S1 Table**. Expression plasmids of coronavirus spike proteins or ACE2 proteins and variants were created by synthesizing fragments by Integrated DNA Technologies (IDT, Coralville, IA, USA), and ligating them into pCAGGS or pcDNA vector respectively using In-Fusion HD Cloning Kit (Takara Bio USA) according to manufacturer’s instructions. ACE2-Fc variants were generated by the QuikChange II site-directed mutagenesis protocol (Agilent). The plasmid expressing human DPP4 is a gift from Dr. Bart L. Haagmans.”

“relative ACE2 expressing levels shown in S1C Fig that determined by an antibody recognizing an amino-terminal myc-tag.”

Article 6:

Pei Li, Ruixuan Guo, Yan Liu, Yingtao Zhang, Jiaxin Hu, Xiuyuan Ou, Dan Mi, Ting Chen, Zhixia Mu, Yelin Han, Zihan Chen, Zhewei Cui, Leiliang Zhang, Xinquan Wang, Zhiqiang Wu, Jianwei Wang, Qi Jin, Zhaohui Qian,

The Rhinolophus affinis bat ACE2 and multiple animal orthologs are functional receptors for bat coronavirus RaTG13 and SARS-CoV-2,

Science Bulletin,
Volume 66, Issue 12,
2021,
Pages 1215-1227,
ISSN 2095-9273,
https://doi.org/10.1016/j.scib.2021.01.011.
(https://www.sciencedirect.com/science/article/pii/S2095927321000475)

Results:

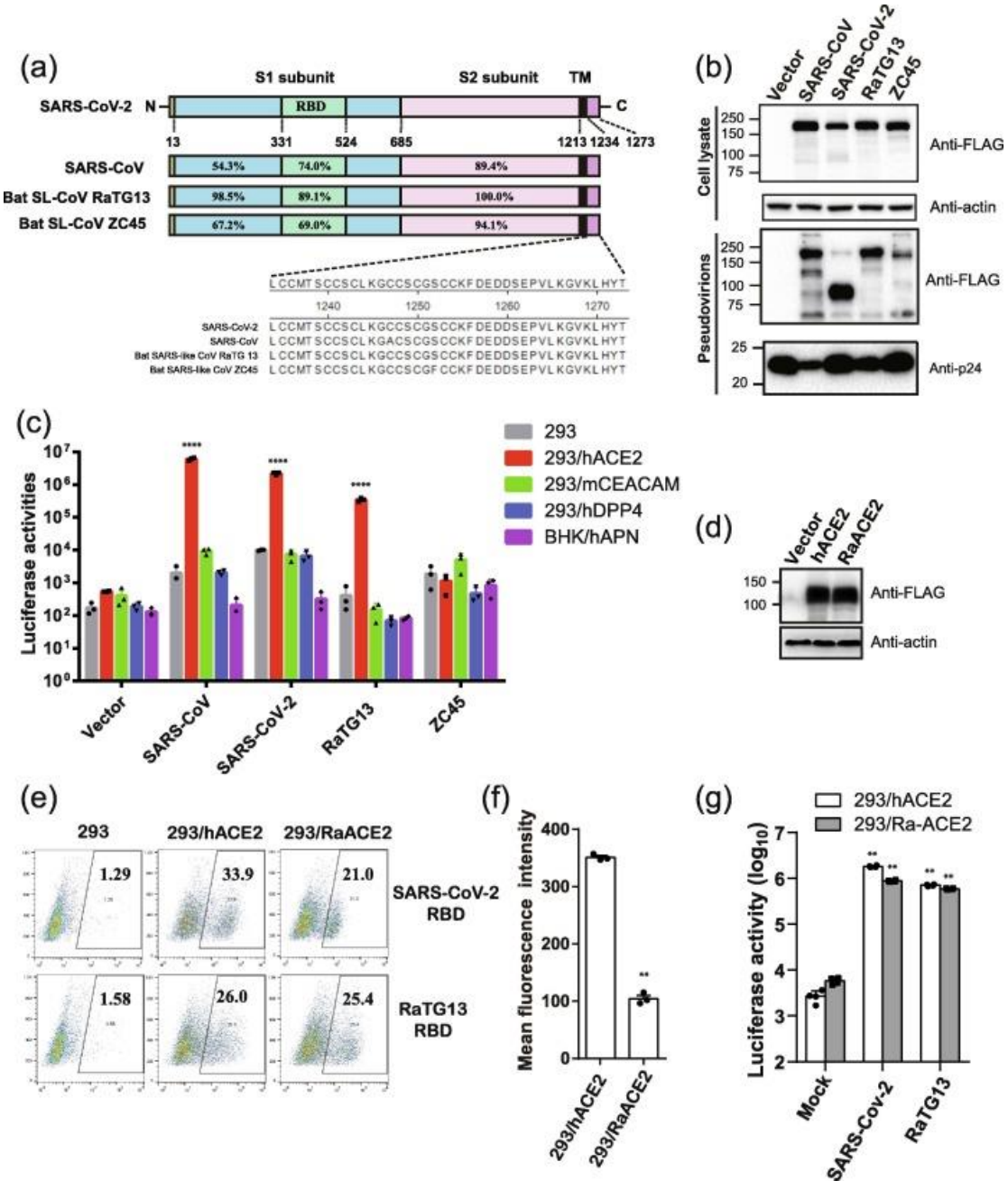

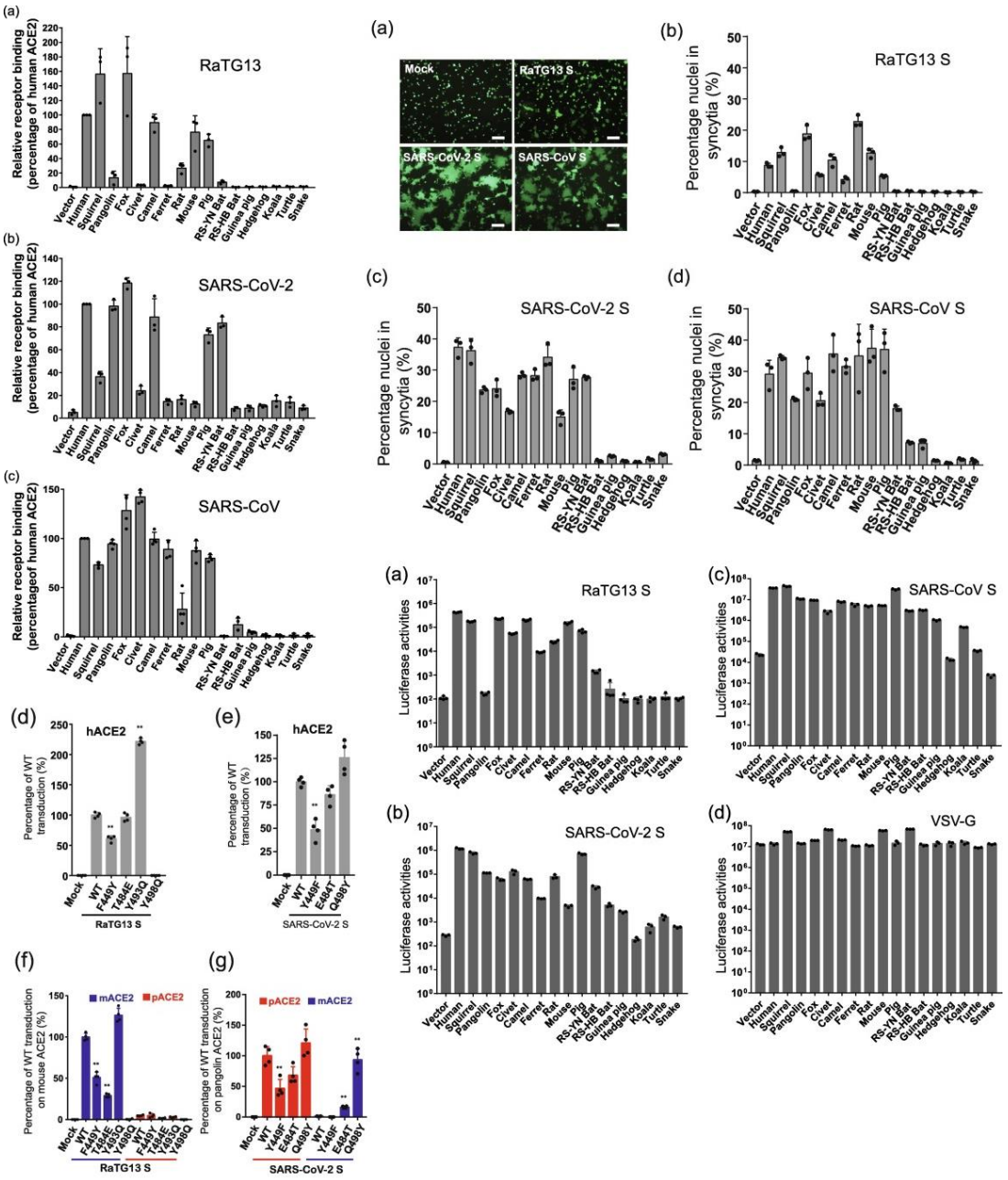

"RaTG13 RBD also demonstrated slightly weaker binding to hACE2 than SARS-CoV-2 RBD." "However, RaTG13 RBD only showed very limited binding to pangolin ACE2 (Fig. 3b), its S protein only induced background level of syncytia on HEK293 cells transiently expressing pangolin ACE2 (Fig. 4c), and RaTG13 S pseudovirions also only gave background level of transduction on HEK293 cells transiently expressing pangolin ACE2 (Fig. 5a), indicating that RaTG13 virus might not be able to infect pangolin."

Methods section:

Species	24	27	28	30	31	34	35	37	38	41	42	79	82	83	330	353	354	355	357	393	Accession
Human	Q	T	F	D	K	H	E	E	D	Y	Q	L	M	Y	N	K	G	D	R	R	NP_068576
Squirrel	L	T	F	D	K	Q	E	E	D	H	Q	L	D	Y	N	K	G	D	R	R	XP_026252505
Pangolin	E	T	F	E	K	S	E	E	E	Y	Q	I	N	Y	N	K	H	D	R	R	XP_017505746
Fox	L	T	F	E	K	Y	E	E	E	Y	Q	L	T	Y	N	K	G	D	R	R	XP_025842512
Civet	L	T	F	E	T	Y	E	Q	E	Y	Q	L	T	Y	N	K	G	D	R	R	AAX63775
Camel	L	T	F	E	E	H	E	E	D	Y	Q	T	T	Y	N	K	G	D	R	R	XP_006194263
Ferret	L	T	F	E	K	Y	E	E	E	Y	Q	H	T	Y	N	K	R	D	R	R	NP_001297119
Rat	K	S	F	N	K	Q	E	E	D	Y	Q	I	N	F	N	H	G	D	R	R	NP_001012006
Mouse	N	T	F	N	N	Q	E	E	D	Y	Q	T	S	F	N	H	G	D	R	R	NP_001123985
Pig	L	T	F	E	K	L	E	E	D	Y	Q	I	T	Y	N	K	G	D	R	R	NP_001116542
RA Bat	R	I	F	D	N	H	E	E	D	Y	Q	L	N	Y	N	K	G	D	R	R	QMQ39244
RS-YN Bat	E	M	F	D	K	T	K	E	D	H	Q	L	N	Y	N	K	G	D	R	R	AGZ48803
RS-HB Bat	R	T	F	D	E	S	E	E	N	Y	Q	L	N	Y	N	K	G	D	R	R	ADN93475
Guinea pig	L	I	F	D	E	S	E	E	N	Y	Q	L	N	Y	N	K	N	D	R	R	ACT66270
Deer	Q	T	F	E	K	H	E	E	D	Y	Q	M	T	Y	N	K	G	D	R	R	XP_020768965
Hedgehog	Q	S	F	T	T	N	E	E	N	Y	Q	L	K	F	K	L	N	D	R	R	XP_004710002
Koala	R	E	F	E	T	K	E	E	E	Y	Q	I	T	F	N	K	G	D	R	R	XP_020863153
Turtle	E	N	F	S	E	V	Q	E	D	Y	A	N	K	Y	N	K	K	D	R	R	XP_006122891
Snake	V	K	F	E	Q	A	R	T	D	Y	N	N	M	F	N	K	E	D	R	R	ETE61880

"The cDNAs encoding ACE2 orthologs (Table 1) were synthesized by Sango Biotech (Shanghai, China) and cloned into the pCMV14-3× Flag vector between the HindIII and BamHI sites. All the constructs were verified by sequencing."

Article 7:

Spike mutation T403R allows bat coronavirus RaTG13 to use human ACE2

Fabian Zech, Daniel Schniertshauer, Christoph Jung, Alexandra Herrmann, Qinya Xie, Rayhane Nchioua, Caterina
Prelli Bozzo, Meta Volcic, Lennart Koepke, Jana Krüger, Sandra Heller, Alexander Kleger, Timo Jacob, Karl-Klaus Conzelmann, Armin Ensser, Konstantin
M.J. Sparrer, Frank Kirchhoff

bioRxiv 2021.05.31.446386; doi: https://doi.org/10.1101/2021.05.31.446386

Results:

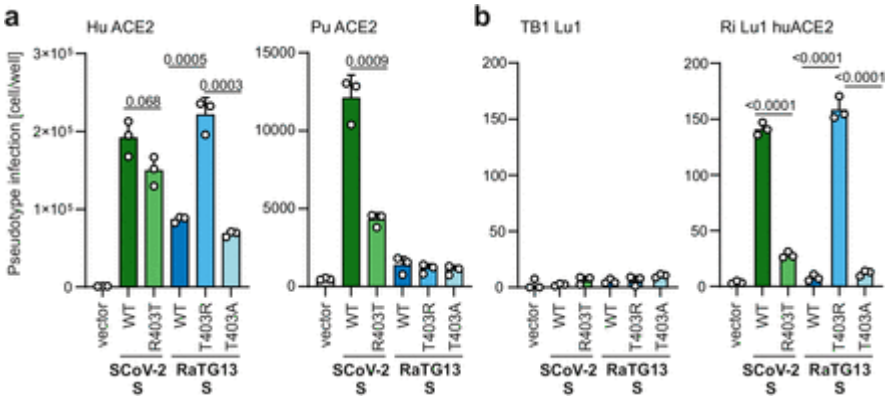

"SARS-CoV-2 S and T403R RaTG13 S allow entry with human but not bat ACE2.

a, HEK293T cells expressing indicated ACE2 (Human ACE2 or *Rhinolophus affinis* ACE2) constructs or **b,** Tb 1 Lu, *Tadarida brasiliensis* derived lung epithelial and Ri 1 Lu huACE2 *Rhinolophus affinis* derived lung epithelial cells expressing human ACE2 were infected with VSVΔG-GFP pseudotyped with SARS-CoV-2, RaTG13 or indicated mutant S. Quantification by automatic counting of GFP positive cells. n=3 (biological replicates) ± SEM. P values are indicated (student's t test)."

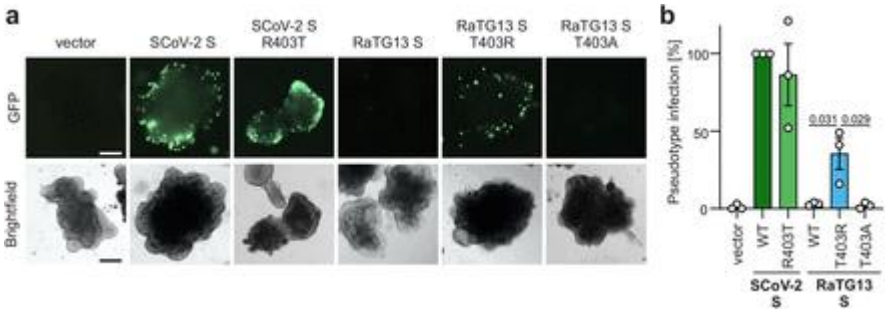

"T403R allows RaTG13 S to mediate infection of human gut organoids.

a, Bright field and fluorescence microscopy (GFP) images of hPSC derived gut organoids infected with VSVΔG-GFP (green) pseudotyped with SARS-CoV-2, RaTG13 or indicated mutant S (300 µl, 2 h). Scale bar, 250µm. **b,** Quantification of the percentage of GFP-positive cells of (a). n=3 (biological replicates) ± SEM. P values are indicated (student's t test)."

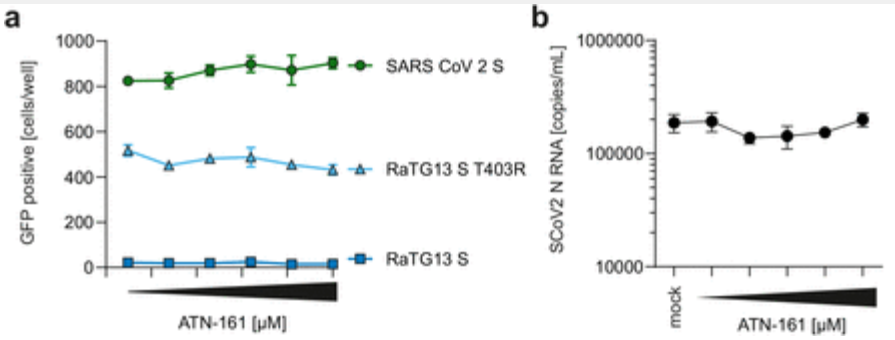

" **a,** Automated quantification by GFP fluorescence of Caco-2 cells preincubated with indicated amounts of α5β5 integrin Inhibitor ATN-161 and infected with VSVΔG-GFP pseudotyped with SARS-CoV-2, RaTG13 T403R mutant or RaTG13 S. n=3 (biological replicates) ± SEM. **b,** Quantification of viral RNA copies in the supernatant of Calu-3 cells

preincubated with indicated amounts of ATN-161 and infected SARS-CoV-2 (MOI 0.05, 6 h). n=3 (biological replicates) ± SEM. P values are indicated (student's t test).”

Methods section:

“Cell culture and viruses
All cells were cultured at 37°C in a 5% CO2 atmosphere. Human embryonic kidney 293T cells purchased from American type culture collection (ATCC: #CRL3216) were cultivated in Dulbecco's Modified Eagle Medium (DMEM, Gibco) supplemented with 10% (v/v) heat-inactivated fetal bovine serum (FBS, Gibco), 2 mM L-glutamine (PANBiotech), 100 µg/ml streptomycin (PANBiotech) and 100 U/ml penicillin (PANBiotech). Calu-3 (human epithelial lung adenocarcinoma, kindly provided and verified by Prof. Frick, Ulm University) cells were cultured in Minimum Essential Medium Eagle (MEM, Sigma) supplemented with 10% (v/v) FBS (Gibco) (during viral infection) or 20% (v/v) FBS (Gibco) (during all other times), 100 U/ml penicillin (PAN-Biotech), 100 µg/ml streptomycin (PAN-Biotech), 1 mM sodium pyruvate (Gibco), and 1 mM NEAA (Gibco). Caco-2 (human epithelial colorectal adenocarcinoma, kindly provided by Prof. Holger Barth, Ulm University) cells were cultivated in DMEM (Gibco) containing 10% FBS (Gibco), 2 mM glutamine (PANBiotech), 100 µg/ml streptomycin (PANBiotech), 100 U/ml penicillin (ANBiotech), 1 mM Non-essential amino acids (NEAA, Gibco), 1 mM sodium pyruvate (Gibco). I1-Hybridoma cells were purchased from ATCC (#CRL-2700) and cultured in RPMI supplemented with 10% (v/v) heat-inactivated FBS (Gibco), 2 mM L-glutamine (PANBiotech), 100 µg/ml streptomycin (PANBiotech) and 100 U/ml penicillin (PANBiotech). Tb 1 Lu (Tadarida brasiliensis derived lung epithelial) and Ri 1 Lu huACE2 (Rhinolophus affinis derived lung epithelial cells expressing human ACE2, ACE2, kindly provided by Marcel A. Müller, were cultured in DMEM supplemented with 10% (v/v) heat-inactivated FBS (Gibco), 2 mM L-glutamine (PANBiotech), 100 µg/ml streptomycin (PANBiotech) and 100 U/ml penicillin (PANBiotech), 2 mM sodium pyruvate (Gibco). Viral isolate BetaCoV/France/IDF0372/2020 (#014V-03890) was obtained through the European Virus Archive global.”

Article 8:

Wrobel, A.G., Benton, D.J., Xu, P. *et al.* Structure and binding properties of Pangolin-CoV spike glycoprotein inform the evolution of SARS-CoV-2. *Nat Commun* **12,** 837 (2021). https://doi.org/10.1038/s41467-021-21006-9

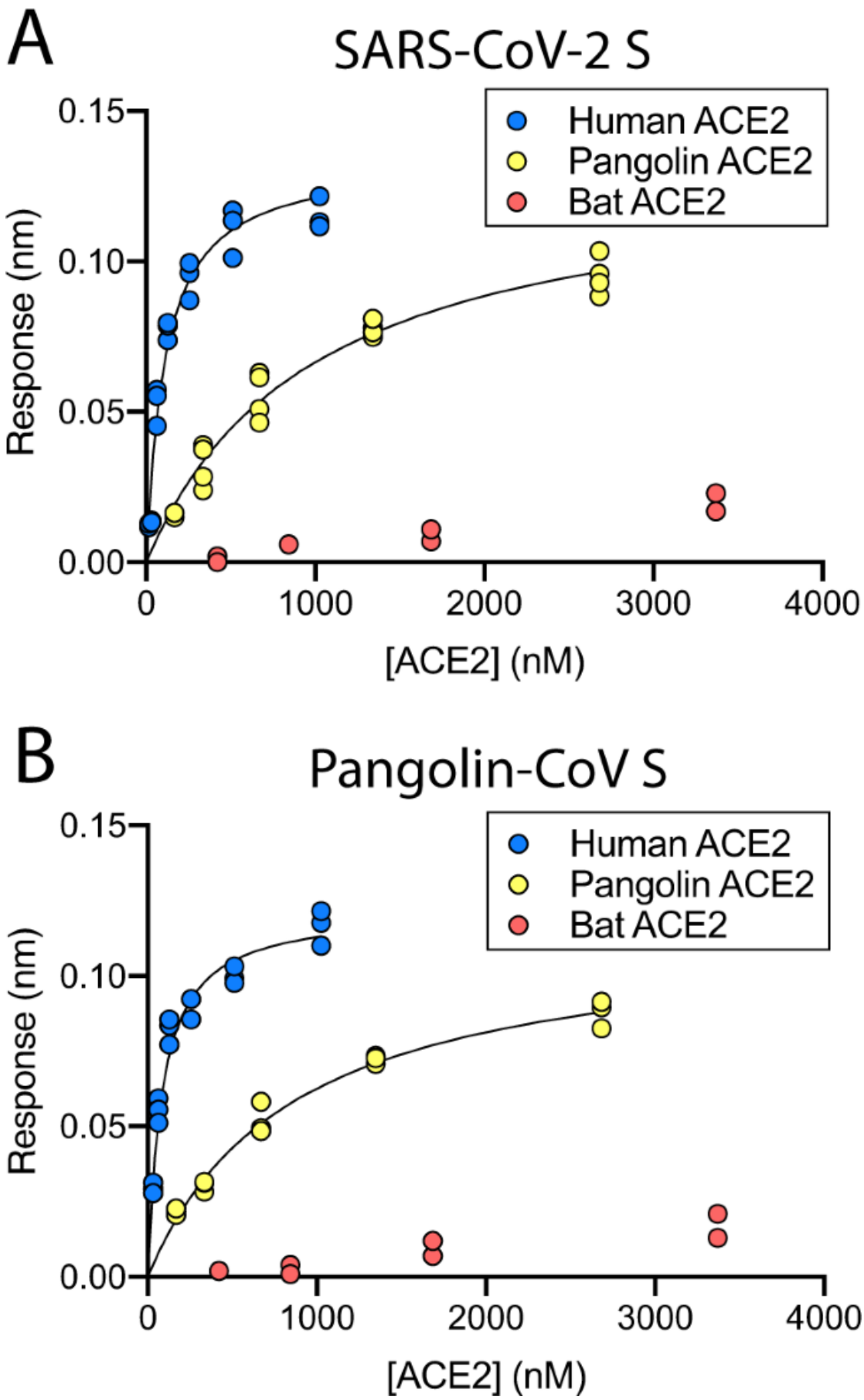
A
SARS-CoV-2 S
Human ACE2
Pangolin ACE2
Bat ACE2
Response (nm)
0.15
0.10
0.05
0.00
0
1000
2000
3000
4000
[ACE2] (nM)
B
Pangolin-CoV S
Human ACE2
Pangolin ACE2
Bat ACE2
Response (nm)
0.15
0.10
0.05
0.00
0
1000
2000
3000
4000
[ACE2] (nM)

Results:

“To characterise the pangolin virus spike and compare it with that of SARS-CoV-2, we expressed and purified two different Pangolin-CoV spike ectodomains. These are based on the sequences of viruses isolated from pangolins seized in China’s Guangdong province in 20198,9. We also produced recombinant ectodomains of ACE2 proteins from human, bat (Rhinolophus ferremequinum) and pangolin in order to perform comparative biolayer interferometry assays. Both pangolin proteins (referred to as Pangolin-CoV S and Pangolin-CoV S’) showed strong (<100 nM) binding to the human ACE2, approximately ten-fold weaker binding to pangolin ACE2, and very weak binding to bat ACE2 (Fig. 1A and Supplementary Fig. 1).”

Spike	ACE2	K_d amplitude (nM)	K_d kinetics (nM)
SARS-CoV-2	Human	110 ± 14.7	75.5 ± 12.9
	Pangolin	987 ± 112	896 ± 225
Pangolin-CoV	Human	74.0 ± 13.0	42.1 ± 10.0
	Pangolin	850 ± 169	663 ± 139

Equilibrium dissociation constants determined from the analysis of the data in Fig. 1 (K_d Amplitude) compared with values determined from analysis of the corresponding kinetic data (K_d Kinetics) (see Fig. S1).

“None of the three species of ACE2 were bound strongly by the bat virus RaTG13 S. This observation correlates with the substantial sequence differences between the RBD of RaTG13 and the RBDs of spike proteins from the viruses of the other two species (Table 2).”

Methods section:

“The construct coding for the human ACE2 ectodomain (residues 1–615, NCBI reference NM_021804.2) was codon optimised and made with a C-terminal Twin-strep tag preceded by a DYK-tag and cloned into pcDNA.3.1(+) by GenScript. The ACE2 ectodomains (residues 19–615) from the Malayan pangolin (Manis javanica, NCBI reference XP_017505746.1) and an archetypal horseshoe bat species, Greater horseshoe bat (Rhinolophus ferremequinum, Uniprot reference B6ZGN7) were also cloned by Genscript into pcDNA.3.1(+) with the same tags as described before for the human ACE26 viz. DYK plus Twin-strep tag at the C-terminus and the secretion leader sequence derived from Ig-kappa at the N-terminus.”

Article 9:

Tyler N. Starr, Allison J. Greaney, Sarah K. Hilton, Daniel Ellis, Katharine H.D. Crawford, Adam S. Dingens, Mary Jane Navarro, John E. Bowen, M. Alejandra Tortorici, Alexandra C. Walls, Neil P. King, David Veesler, Jesse D. Bloom,
Deep Mutational Scanning of SARS-CoV-2 Receptor Binding Domain Reveals Constraints on Folding and ACE2 Binding,
Cell,
Volume 182, Issue 5,
2020,

Pages 1295-1310.e20,
ISSN 0092-8674,
https://doi.org/10.1016/j.cell.2020.08.012.
(https://www.sciencedirect.com/science/article/pii/S0092867420310035)

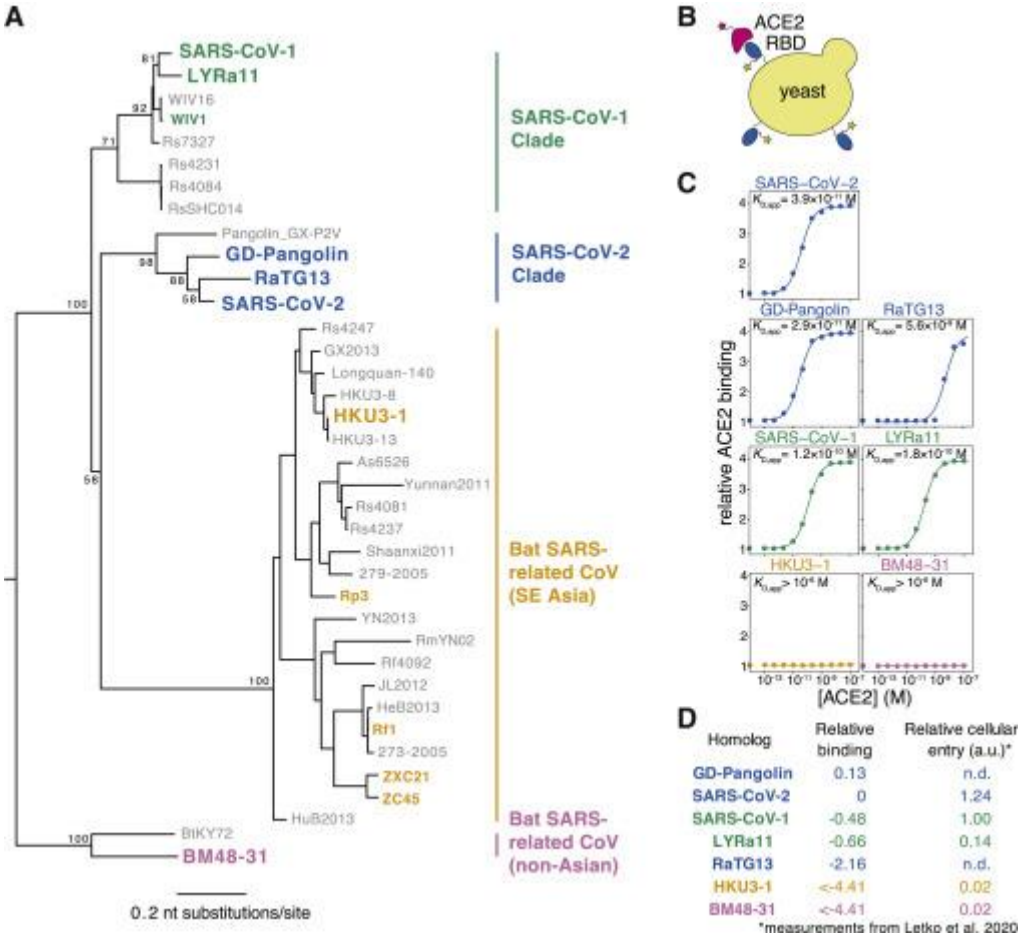

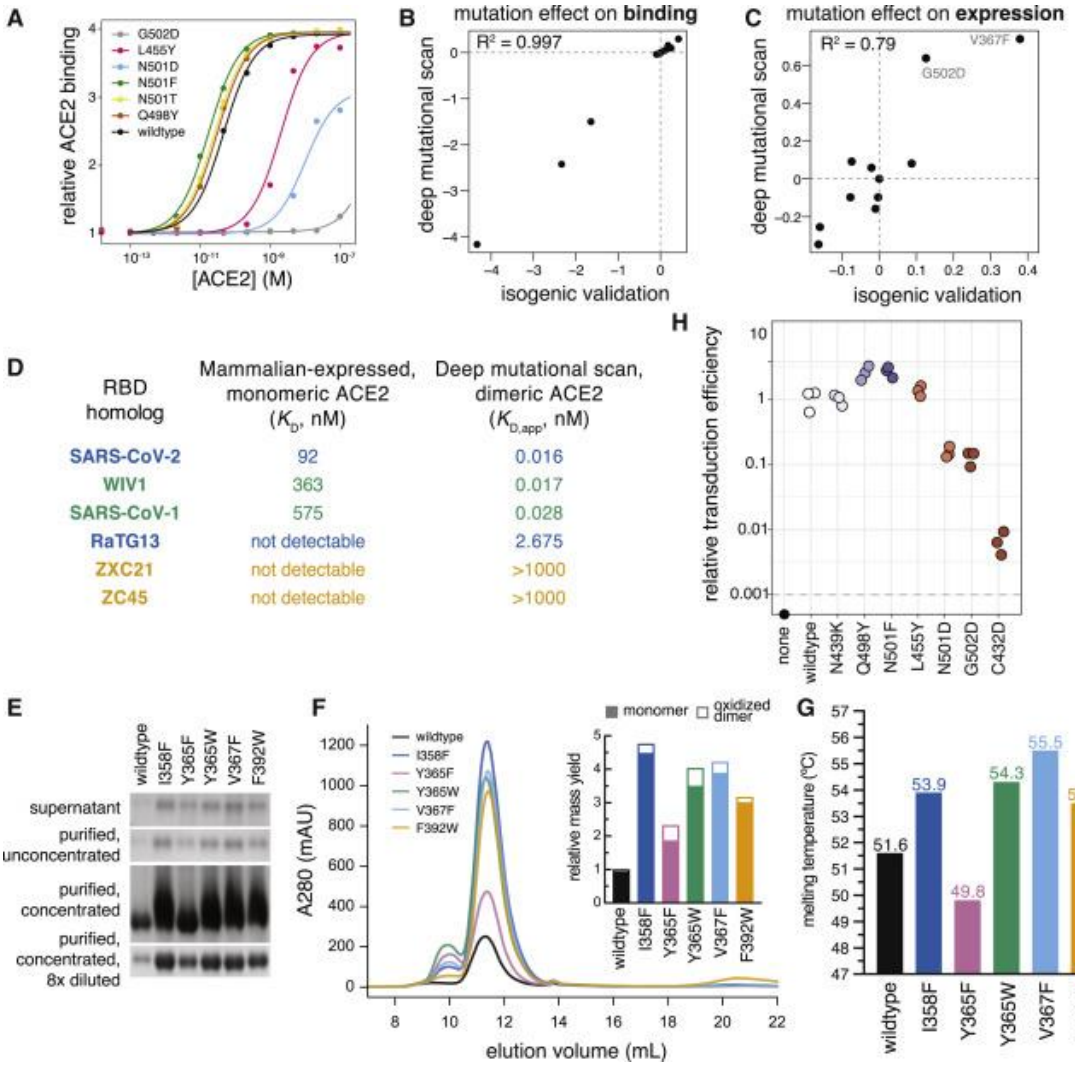
A
relative ACE2 binding
G502D
L455Y
N501D
N501F
N501T
Q498Y
wildtype
[ACE2] (M)
B
mutation effect on binding
R² = 0.997
deep mutational scan
isogenic validation
C
mutation effect on expression
R² = 0.79
V367F
G502D
deep mutational scan
isogenic validation
D
RBD homolog
Mammalian-expressed, monomeric ACE2 (K_D, nM)
Deep mutational scan, dimeric ACE2 ($K_{D,app}$, nM)
SARS-CoV-2 92 0.016
WIV1 363 0.017
SARS-CoV-1 575 0.028
RaTG13 not detectable 2.675
ZXC21 not detectable >1000
ZC45 not detectable >1000
H
relative transduction efficiency
none
wildtype
N439K
Q498Y
N501F
L455Y
N501D
G502D
C432D
E
wildtype
I358F
Y365F
Y365W
V367F
F392W
supernatant
purified, unconcentrated
purified, concentrated
purified, concentrated, 8x diluted
F
wildtype
I358F
Y365F
Y365W
V367F
F392W
A280 (mAU)
elution volume (mL)
monomer
oxidized dimer
relative mass yield
G
melting temperature (°C)
51.6
53.9
49.8
54.3
55.5
53.5
wildtype
I358F
Y365F
Y365W
V367F
F392W

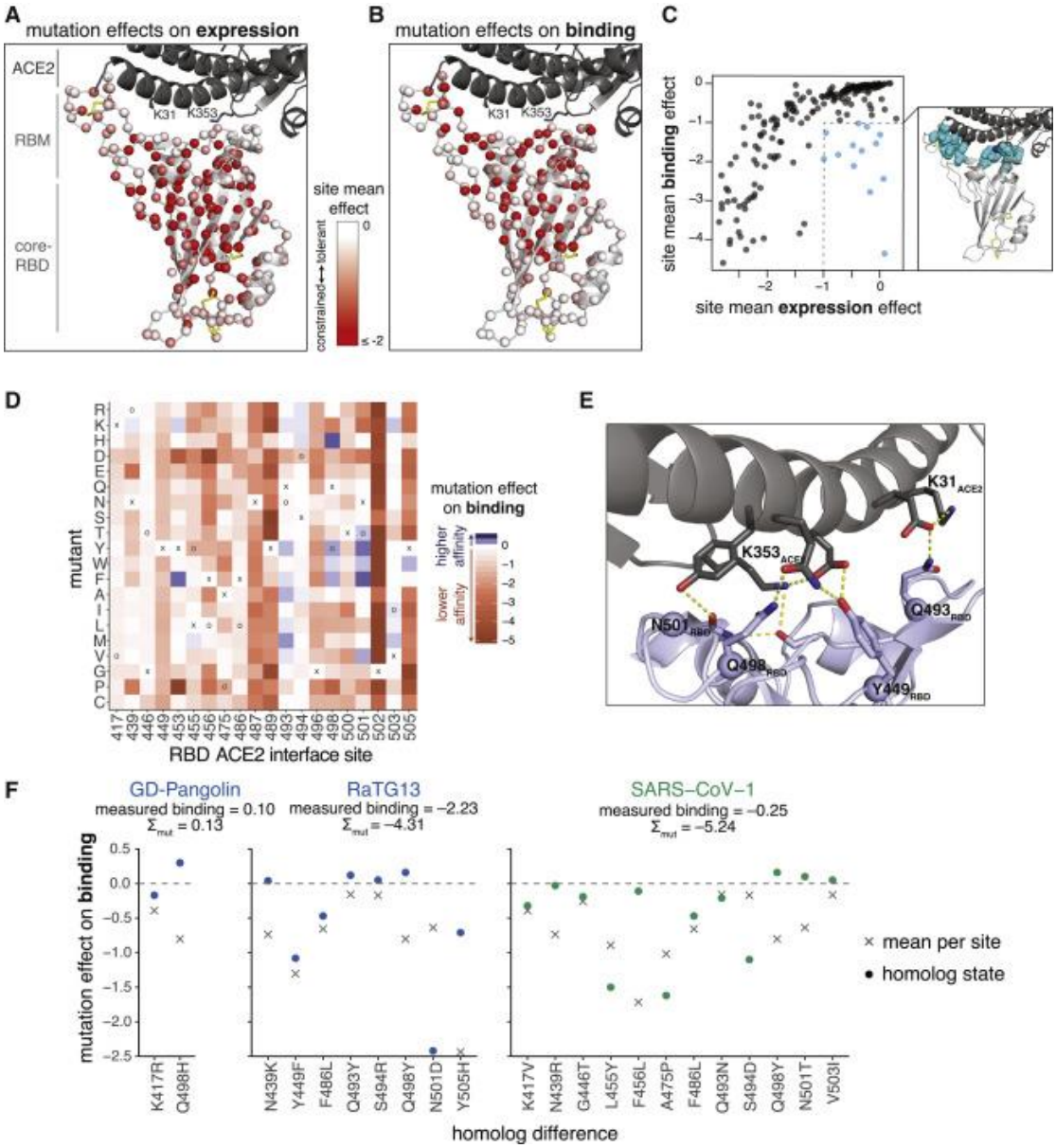

Results:

"For example, GD-Pangolin has higher affinity for ACE2 than SARS-CoV-2 (Figures 1C and 2D), and this can be explained by the affinity-enhancing Q498H mutation present in this virus's RBD sequence (Figure 5F). In contrast, RaTG13 has substantially lower affinity for ACE2 than SARS-CoV-2 (Figures 1C and 2D), consistent with the presence of affinity-decreasing mutations including Y449F and N501D (Figure 5F)."

Methods section:

Chemicals, Peptides, and Recombinant Proteins		
Biotinylated human ACE2	ACROBiosytems	Cat# AC2-H82E6

Article 10:

Wrobel, A.G., Benton, D.J., Xu, P. *et al.* SARS-CoV-2 and bat RaTG13 spike glycoprotein structures inform on virus evolution and furin-cleavage effects. *Nat Struct Mol Biol* **27,** 763–767 (2020). https://doi.org/10.1038/s41594-020-0468-7

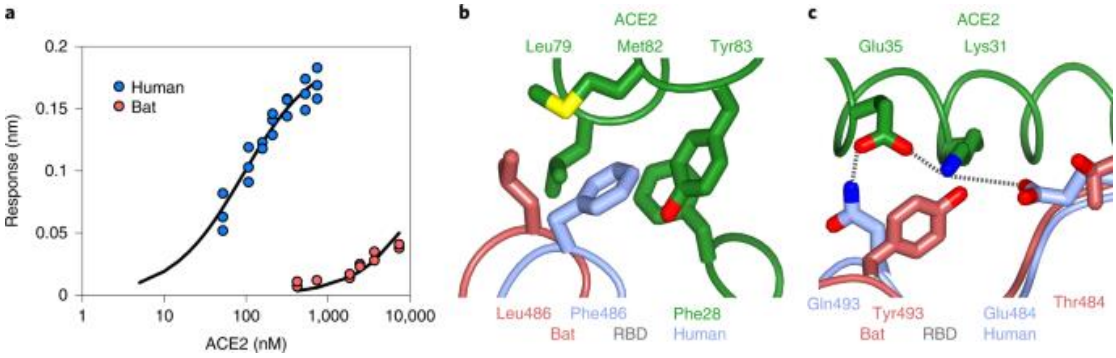

Results:

"Amplitude analysis suggested that SARS-CoV-2 S binds approximately 1,000 times more tightly to ACE2 than the bat virus protein does, with Kd values of <100 nM and >40 μM, respectively (Fig. 3a)."

"Although the overall structures of human and bat virus S proteins are similar, there are key differences in their properties, including a more stable precleavage form of human S and about 1,000-fold tighter binding of SARS-CoV-2 to human receptor."

Methods section:

"The ectodomain (residues 19–615) of human ACE2 (NM_021804.2) was optimized for human expression, synthesized and cloned into pcDNA.3.1(+) vector by GenScript with an N-terminal Ig-kappa chain secretion leader sequence and a C-terminal Twin-Strep tag preceded by a DYK tag."

Discussions:

Rhinolophus Affinis ACE2 alleles and ACE2 accession numbers:

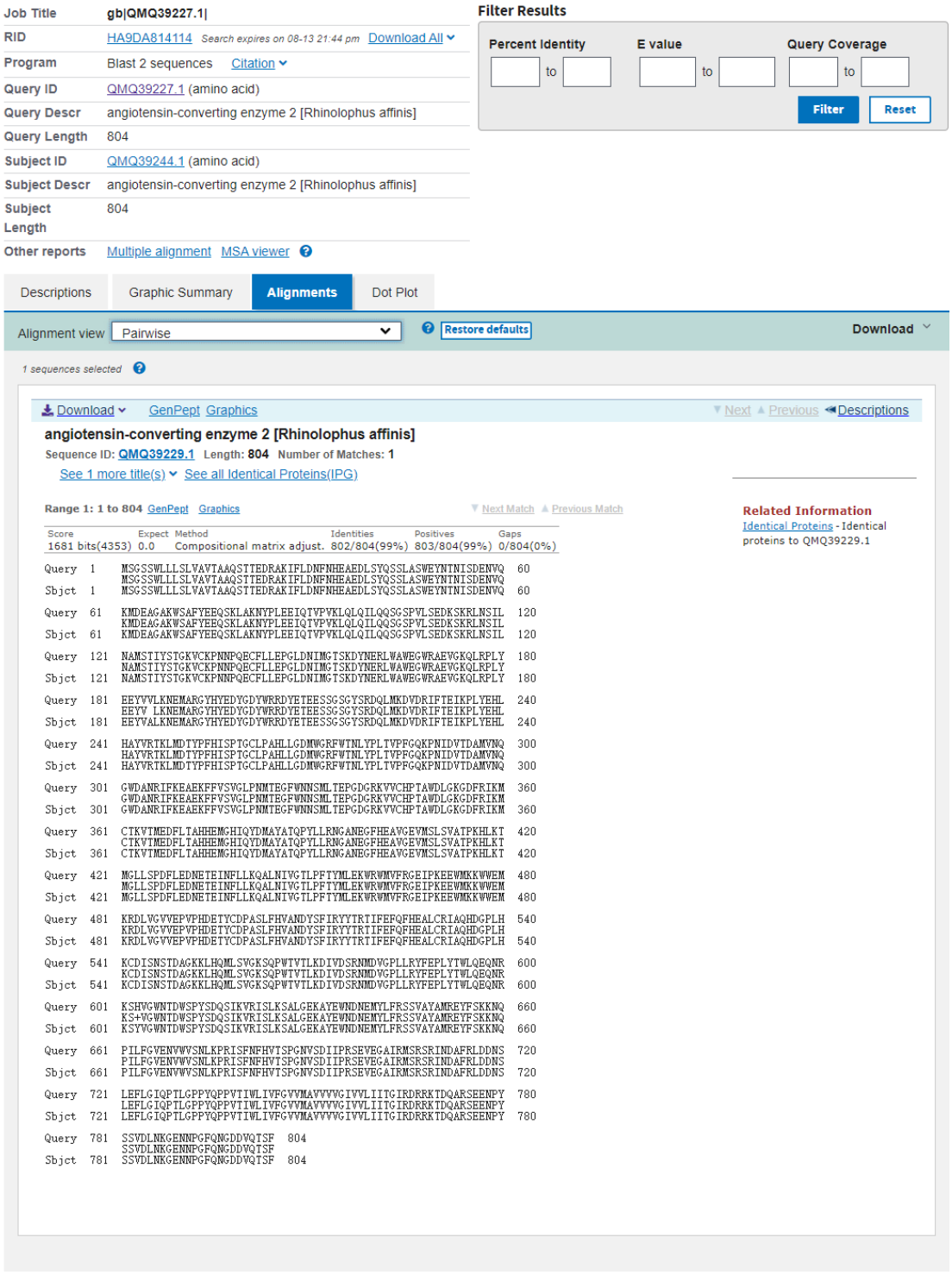

Figure 2: The Rhinolophus Affinis ACE2 allele 9479(QMQ39227.1,MT394208.1) have no difference with the allele 4331(QMQ39244.1, MT394225.1) on the site where the ACE2 interact

with the RBD.

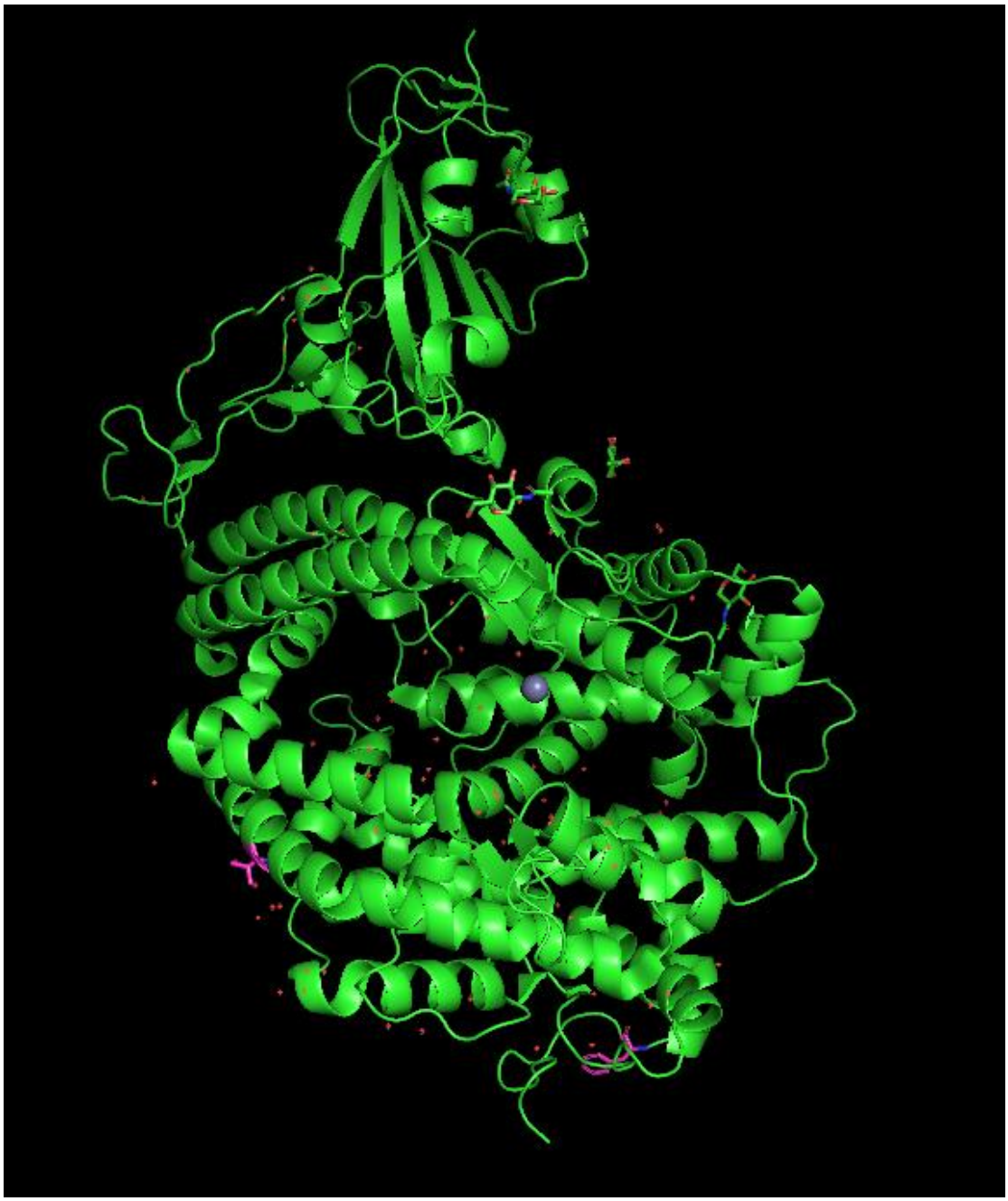

Figure 3: The sites where Rhinolophus Affinis ACE2 allele 9479 and 4331 differs from each other. Both amino acids were located on the surface of the ACE2 that is distal to the RBD binding site.

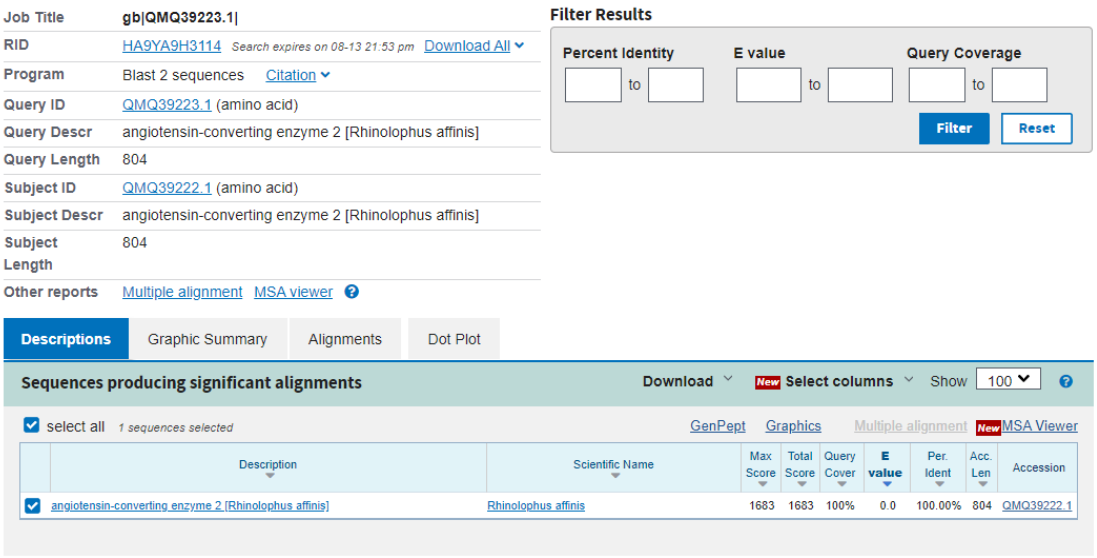

Figure 4:

The Protein sequence of QMQ39223.1(MT394204.1) and Rhinolophus Affinis ACE2 allele 787(QMQ39222.1, MT394203.1) are identical to each other.

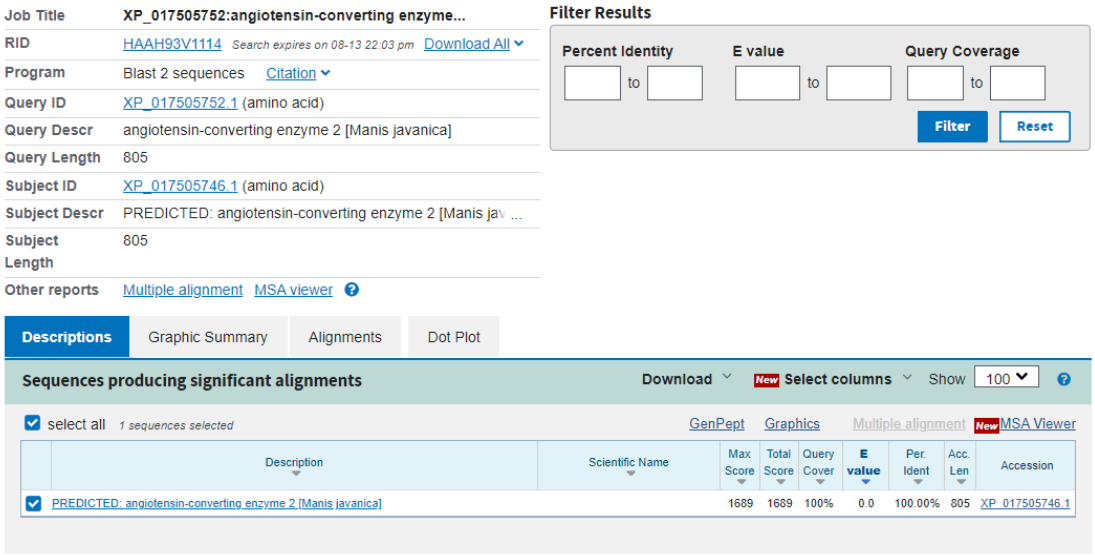

Figure 5: The two M.javanica ACE2 accessions XP_017505752.1 and XP_017505746.1 are identical to each other.

Two distinct binding properties for ACE2 expressed with different Methodologies.

"GS" identified on the N-terminus of the mature ACE2 ectodomains use in article 1 and article 3.

For Article 1, the R.affinis ACE2 was expressed as 19-615 that was cloned into pUPE.107.03[1] using 5'-BamHI and 3'-NotI sites, which, according to the methods section of [1] where "All constructs were obtained via polymerase chain reaction using Mus musculus (mouse) Olfm1 BMZ isoform (NCBI Reference Sequence NP_062371) cDNA IRAVp968C0174D (Source Bioscience) as a template. They were subsequently subcloned using BamHI and NotI restriction sites into the pUPE107.03 (U-Protein Express) mammalian expression vector containing an Epstein-Barr virus origin of replication, a C-terminal His6-tag and a cystatin signal peptide for secretion.", the resulting protein products "are flanked by an N-terminal GS- and a C-terminal -AAAHHHHHH sequence in the mature protein as a result of the restriction sites and affinity tag."[1]

The human ACE2, likewise, was "amplified using PCR with oligonucleotides hACE2ecto-Fw (5'-aaaatgatcaTCCACCATTGAGGAACAGGCC-3') and hACE2ecto_Rv (5'-aaaagcggccgcGTCTGCATATGGACTCCAGTC-3') and sub-cloned into a pUPE.06.45 expression vector (U-Protein Express B.V., The Netherlands) providing the signal sequence from cystatin followed by a removable (TEV-cleavable) N-terminal 6xHis-Strep-tag."

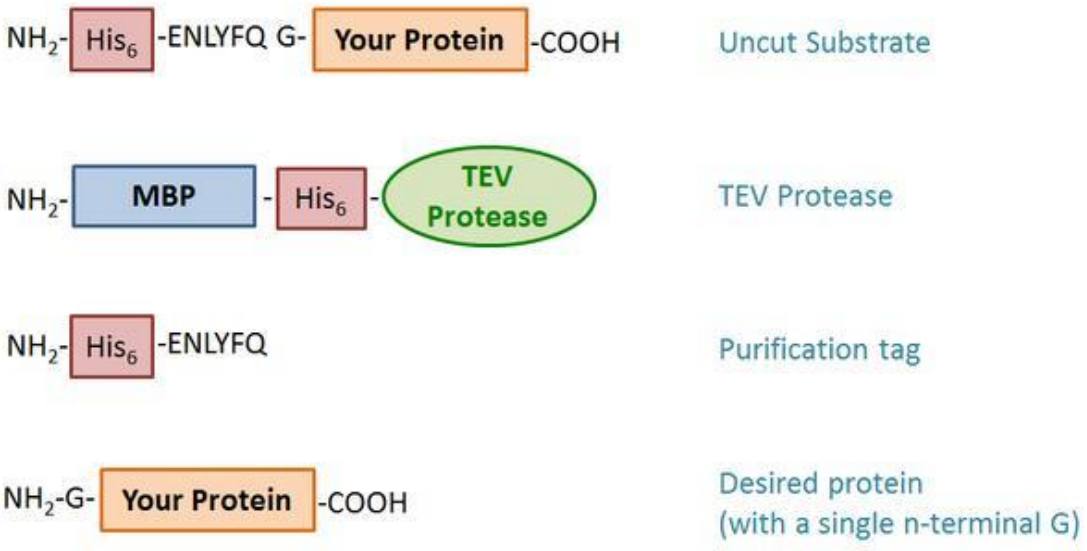

Figure 6[2]: The cleavage site for the TEV protease.

By translating the forward primer sequence using ExPaSy Translate tool, the sequence is revealed to align to the AA 19 for the human ACE2 mRNA, and encodes a single BclI restriction site(T^GATCA) immediately before the 5' end.

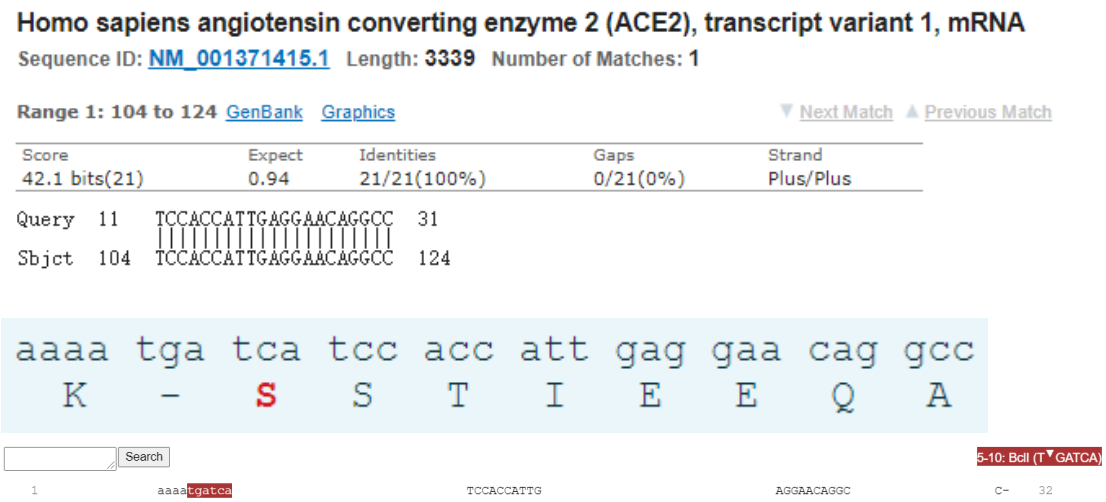

Figure 7a: Alignment, translation and restriction mapping analysis of the forward ACE2 primer used by article 1. A BclI site can be seen leaving behind an overhang of 5'-GATC-3'.

Figure 7b: the cut site of BamHI, according to [3].

The overhang of GATC was found to be compatible with BamHI, which encodes the amino acid sequence "GS" when translated.

As the hACE2 cDNA is found to require restriction-ligation based cloning in order to be inserted into a cloning vector that have additional translated amino acid sequences before it, as the TEV protease can only cut at site ENLYFQ^G, and the BclI site encodes a premature stop codon which prevent the same enzyme from being used for the preparation of the linearized expression vector for the purpose of ligation, the only possible cut site is at the very beginning of the "GS", which lead to the same additional "GS" sequence being inserted into the N-terminus of the mature ACE2.

Likewise, for article 3, The ACE2 cloning strategy is also specified to use BamHI and XhoI for insertion into the expression vector pcDNA3.1(+), using the ACE2 ectodomain beginning from AA 19. A total of 9 R.sinicus sequences was cloned and characterized. As the murine IgK leader sequence is 63bp in length, the synthesis of this oligomer with the BamHI cloning site before the ATG start codon and homology sequences to the ACE2 after the signal sequence cleavage site is not practical for the purpose of cloning, and therefore the most likely construction of the ACE2 expression plasmids for article 3 (and the reference [15] of article 3) is with a BamHI restriction site directly before the AA 19 of the ACE2 cDNA, and cloning into a vetor that already had the mIgK leader sequence and the S tag inserted.

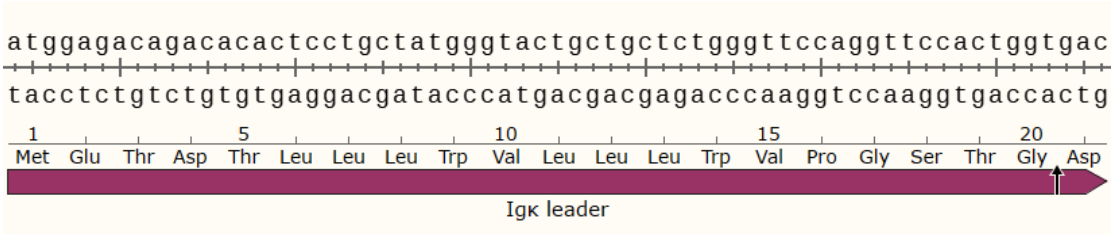

Figure 8a: The murine IgK leader signal sequence.

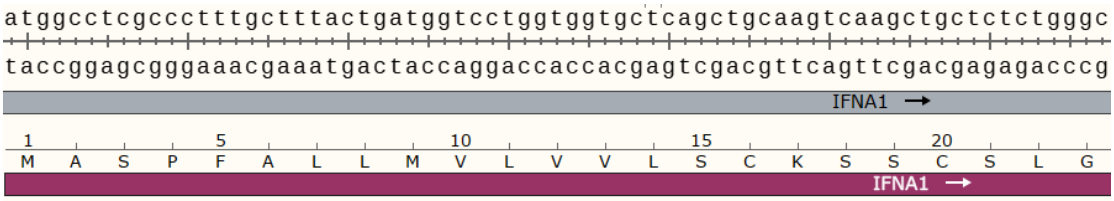

Figure 8b: The human IFNA1 signal sequence.

Similarly, the human Interferon alpha-1 signal sequence, MASPFALLMVLVVLSCKSSCSLG, being 23AA(69bp) in length, is impractical to insert directly into the cloning amplicon as a single primer, and therefore the sequence likely also exist already in the vector backbone and have the BanHI-flanking cDNA sequence cloned into it.

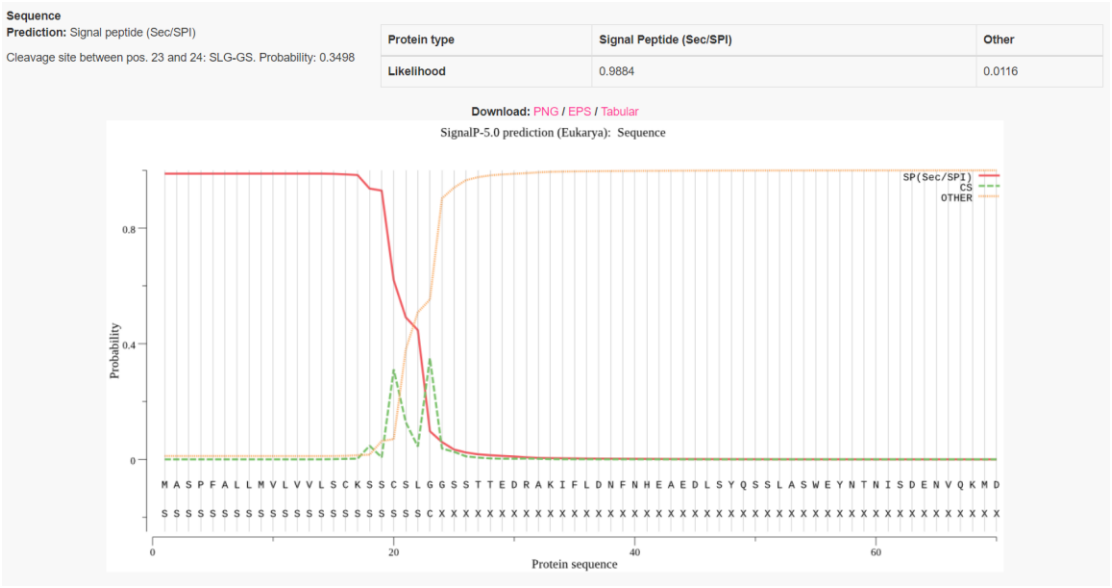

Figure 9: The cleavage site for the hIFNA1 signal peptide sequence, fused to the ectodomain of R.affinis ACE2 at AA 19.

Therefore, for Article 3, the ACE2 is either fused to an N-terminal DGS sequence, or a N-terminal GS sequence, same as in Article 1.

As the result, both Article 1 and article 3 have additional sequences located on the N-terminus of the ACE2, corresponding to the restriction scar sequence of BamHI and BclI, that involves at least one instance of “GS” on the immediate N terminus of the expressed ectodomain.

The native N-terminus of ACE2 is preserved in Article 2,4,6,7.

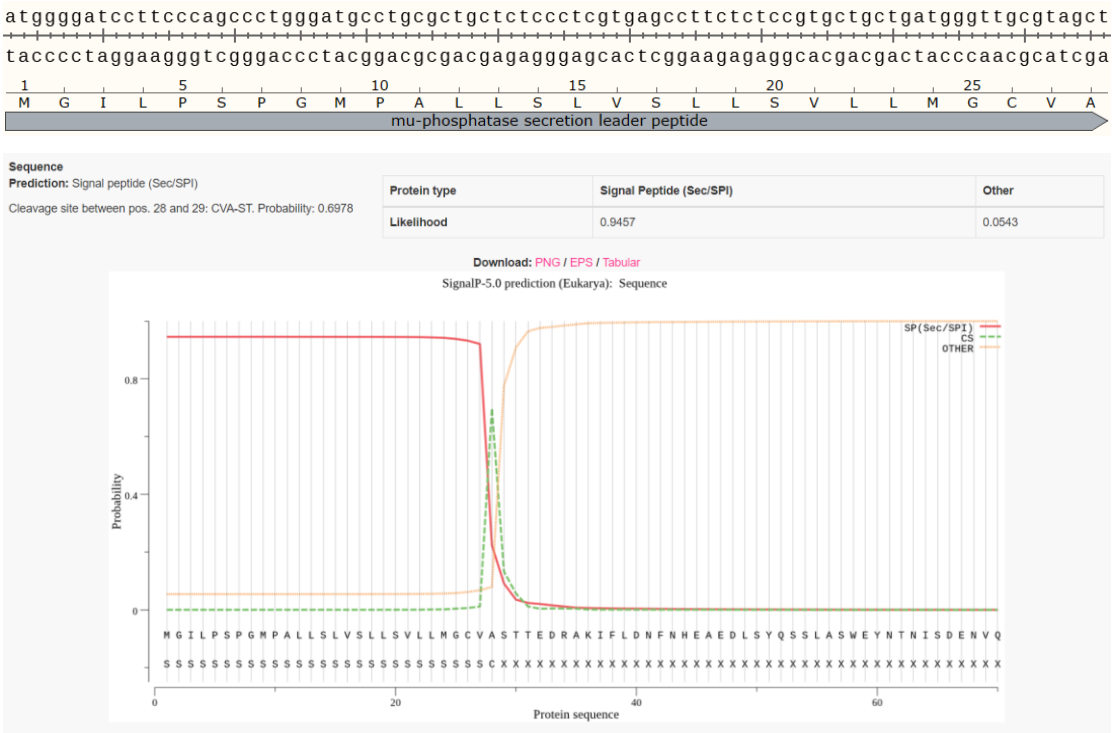

Figure 10: the Mu-Phosphatase signal peptide sequence and cleavage site.

For article 4, the Mu-Phosphatase signal peptide, from pOPIN, was used for the expressed ectodomains for R.affinis ACE2. This signal sequence is cut at the CVA-ST sequence and leave behind the ACE2 ectodomain beginning with AA 19.

For Article 2, the full-length ACE2 and the ectodomain C-terminally fused to Fc was used for the flow cytometry and surface plasmon resonance experiment. The pCAGGS vector backbone by itself does not contain an N-terminal signal peptide, and there were no signal peptide found on the vector. This would require the maintenance of the native ACE2 signal peptide from the cDNA.

For Article 6, the ACE2 (full-length) is synthesized and cloned into the pCMV14-3xflag vector, which carried only 3xFLAG tag on the C-terminus.

For article 7, the ACE2 expression construct is not specified, however, the testing also involved the Rhinolophus Affinis Lung epithelial-derived cell Ri 1 Lu, which failed to permit entry of RaTG13 S pseudotyped VSV even with an exogenous supplementation of human ACE2. As the Ri 1 Lu cells originated from R.affinis, Any endogenous ACE2 expressed within this cell line will have the native signal peptide and cleavage site. As for the CaCo-2 cells and intestinal organoids, as the ACE2 originated from endogenous sources, they carried human ACE2 with the native signal peptide and cleavage site.

A single D is found preceding AA 19 for pACE2 and R.macrotis ACE2 for article 8.

For Article 8, the method section specified residue 1–615 to be used for the expression of hACE2, where the mIgK leader signal sequence was specified for the pACE2 and R.macrotis ACE2. The mIgK leader sequence will leave a single D preceding S19 for the pACE2 and

R.macrotis ACE2.

A single D is found preceding AA 19 for the ACE2 in article 10.

For article 10, the mIgK leader signal sequence will leave behind a single "D" on the N-terminus of the ACE2.

A single Q is found preceding AA19 for the ACE2 used in Article 9.

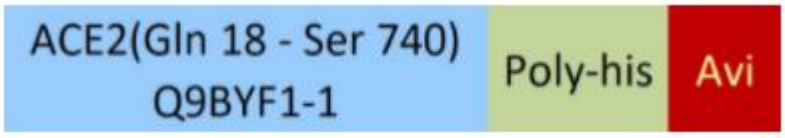

Figure 11: The AcroBioSystem Cat# AC2-H82E6 protein.[4]
Cat# AC2-H82E6 from AcroBioSystems begins with Q18 of hACE2.[4]

A N-terminal C-myc tag is specified in article 5.

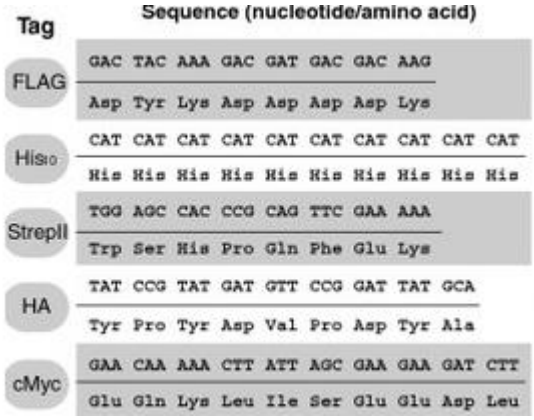

Figure 12: the nucleotide sequences of the FLAG, His10, StrepII, HA and cMyc tags.[5]
An antibody recognizing an N-terminal C-myc tag, EQKLISEEDL, was specified for the purpose of characterizing the expression level of ACE2. This is likely going to distort the RBD binding affinity for the ACE2 constructs specified, in ways that is mostly unpredictable due to the large size of the peptide.

The presence of the "GS" sequence rescues binding of RaTG13 RBD to R.affinis 787 and M.javanica ACE2.

In contrast to articles 4, 5 and 6, detectable binding to R.affinis 787 ACE2 was detected for RaTG13 in Article 3, with transduction efficiency for mpACE2 being similar to hACE2, R.affinis 787 ACE2 being higher than hACE2, and the relative kD for R.affinis 787 and M.javanica ACE2 being only 16.57 and 7.61 times higher than that of SARS-CoV-2 to hACE2.
In article 2, the Kd of RaTG13 to R.affinis 787 ACE2 was determined to be 2354 times higher

compared to SARS-CoV-2 to hACE2.

The presence of the "GS" sequence strongly enhances binding of RaTG13 RBD to human and R.affinis 4331/9479 ACE2.

The binding affinity for RaTG13 RBD to R.affinis 4331 ACE2 was determined to be below that of the binding affinity for RaTG13 RBD to hACE2 for Article 6 (figure 1e,1g), which is significantly lower than that of SARS-CoV-2 to hACE2. The binding affinity for RaTG13 RBD to R.affinis 9479 ACE2 was found to be significantly lower than that of RaTG13 RBD to hACE2 for article 4, which is significantly lower than that of SARS-CoV-2 to hACE2.
In addition, Article 2 found that the binding affinity for RaTG13 RBD to human ACE2 is 182.93 times lower than that of SARS-COV-2 to human ACE2, where article 9 found that the binding affinity for RaTG13 RBD to human ACE2 is 10^-2.16 that of SARS-CoV-2. Article 8 failed to measure the binding for the RaTG13 S to human ACE2, while Article 7 found significantly reduced infection efficiency for RaTG13 S to human ACE2 on HEK293T cells, and little to no infectivity for the same S on CaCo-2 cells using pseudotyped VSV, and no infectivity at all for Human Intestinal Organoid and R.affinis Lung cells. In addition, it was found that the SARS-CoV-2 ΔS replicon system, unlike the pseudovirus system, does not lead to infection on even HEK293T cells using RaTG13 S.

This is in contradiction with Article 1, which claimed that for both human and R.affinis 4331 ACE2, RaTg13 RBD achieved higher binding affinity than SARS-CoV-2, and it is found that the deficit in binding for Article 3 is significantly lower (only ~3.26 times higher Kd for RaTG13 RBD/hACE2 compared to SARS-CoV-2 RBD/hACE2, while Article 2 and 9 have reported Kd that are from 144.54 to 182.93 times higher). Article 10 reported an almost 1000-fold increase in Kd for RaTG13 RBD-hACE2. This corresponds to the fact that while Article 1 have "GS" appended to the N-terminus of the ACE2, Article 3 may have contained an additional "D" in before the "GS".

Interestingly, while the RaTG13 RBD-hACE2 complex can be crystalized as in article 2 and article 1, neither article have generated crystal structures for the R.affinis ACE2 and RaTG13 RBD. This is a likely result of a N-terminal tag-specific, rather than an a1-helix-encompassing, binding mode of the RaTG13 RBD to N-terminal GS-tagged ACE2 molecules (which lead to structures that are too flexible to crystalize properly).

Conclusions:

Using data from 10 different articles on RaTG13 and ACE2 binding, it was found that an addition of the sequence "GS", to the N-terminus of Human, pangolin, R.affinis 787 and R.affinis 9479 ACE2 lead to significantly improved binding affinity to the RaTG13 S or RBD protein compared to that native state of the ACE2 N-terminus, while addition of other sequences lead to little to no increase in binding affinity to the RaTG13 RBD. As the sequence "GS", the result of a restriction scar from BamHI, is absent from the native N-terminus of ACE2

from any mammalian species, This specific enhancement of the RaTg13 binding to ACE2 likely indicate the use of a cloned ACE2, in the methodology that is similar to [15], with additional sequences on the N terminus of the ACE2, during the serial passage attenuation of RaTG13, adapting it for cell culture production. As per article 1, the native signal peptide and it's cleavage site is absent from SRR11085797, which leaves a possibility that a cloned or otherwise stably expressed ACE2 is likely in use, with the addition of the "GS" sequence on the N terminus of the mature ACE2, and the consequent adaptation for the recognition of this specific restriction scar sequence of the RaTg13 RBD.

References

[1] Pronker, M.F., van den Hoek, H. & Janssen, B.J.C. Design and structural characterisation of olfactomedin-1 variants as tools for functional studies. BMC Mol and Cell Biol 20, 50 (2019). https://doi.org/10.1186/s12860-019-0232-1

[2] https://www.geneandcell.com/products/tev-protease

[3] https://www.nebiolabs.com.au/products/r0136-bamhi

[4] https://www.acrobiosystems.com/P3102-Biotinylated-Human-ACE2--ACEH-Protein-HisAvitag%E2%84%A2-%28MALS-verified%29.html

[5] https://www.addgene.org/55183/

[15] Guo H, Hu B-J, Yang X-L, et al. Evolutionary arms race between virus and host drives genetic diversity in bat severe acute respiratory syndrome-related coronavirus spike genes. J Virol. 2020;94(20): e00902–20.